
CLEAR: Calibrated Learning for Epistemic and Aleatoric Risk

Ilia Azizi^{1*} Juraj Bodik^{1,2*} Jakob Heiss^{2*} Bin Yu^{2,3}

¹Department of Operations, HEC, University of Lausanne, Switzerland

²Department of Statistics, University of California, Berkeley, USA

³Department of Electrical Engineering and Computer Science, University of California, Berkeley

*Equal contribution

first.last@unil.ch, jakob.heiss@berkeley.edu, binyu@berkeley.edu

Abstract

Accurate uncertainty quantification is critical for reliable predictive modeling, especially in regression tasks. Existing methods typically address either aleatoric uncertainty from measurement noise or epistemic uncertainty from limited data, but not necessarily both in a balanced way. We propose CLEAR, a calibration method with two distinct parameters, γ_1 and γ_2 , to combine the two uncertainty components for improved conditional coverage. CLEAR is compatible with any pair of aleatoric and epistemic estimators; we show how it can be used with (i) quantile regression for aleatoric uncertainty and (ii) ensembles drawn from the Predictability–Computability–Stability (PCS) framework for epistemic uncertainty. Across 17 diverse real-world datasets, CLEAR achieves an average improvement of 28.2% and 17.4% in the interval width compared to the two individually calibrated baselines while maintaining nominal coverage. This improvement can be particularly evident in scenarios dominated by either high epistemic or high aleatoric uncertainty. Code: <https://github.com/Unco3892/clear>

1 Introduction

Uncertainty quantification is essential for building reliable machine learning systems [1, 2]. Despite their impressive capabilities, modern machine learning methods can give a false sense of reliability; therefore, producing valid prediction intervals remains an open problem. Calibration [3] and conformal methods [4–9] adjust prediction intervals to obtain marginal coverage (that is, covering a certain percentage of the data on average). However, they may suffer from poor conditional coverage, meaning well-calibrated coverage at the individual or subgroup level [10]. In particular, under distribution shift or model misspecification, conditional coverage can degrade substantially, especially in extrapolation regions. Most conformal methods, such as conformalized quantile regression (CQR) [9], only capture aleatoric uncertainty while ignoring epistemic uncertainty.

It is important to distinguish between the two main sources of uncertainty, namely epistemic and aleatoric. Epistemic uncertainty [11] arises from our limited understanding of the data generation process and the model, encompassing issues related to data collection, preprocessing, transformation, and model specification. Notably, this uncertainty is typically large in extrapolation regions where training data is sparse. In contrast, aleatoric uncertainty [12] reflects the inherent variability within the data (stemming from measurement errors, missing covariates, randomness, or intrinsic noise) that cannot be reduced simply by gathering more observations or refining the model unless the data acquisition process itself is improved where more features are measured. Separating the two sources can be beneficial for various applications [13, 14]. For instance, in active learning, epistemic uncertainty helps in selecting which samples to label, while aleatoric uncertainty is less relevant

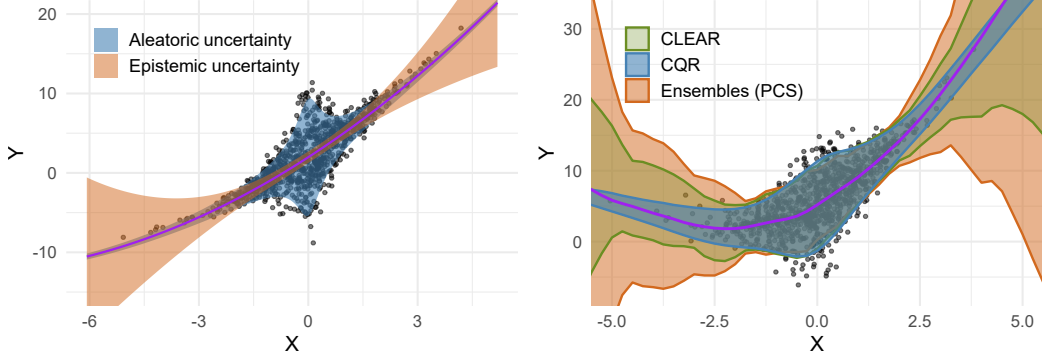


Figure 1: **Left:** Blue represents aleatoric uncertainty, which reflects randomness inherent in the data such as measurement noise. Red represents epistemic uncertainty, which arises from limited sample size. **Right:** Estimated prediction sets using the CLEAR method, which combines both sources of uncertainty in a data-driven manner.

[15]. However, for prediction tasks, appropriately combining both epistemic and aleatoric parts is necessary to account for the overall uncertainty in the model’s predictions [16].

In this work, we contribute to the existing literature by combining aleatoric and epistemic uncertainties in a data-driven manner. We consider prediction intervals $C(x)$ of the form

$$C(x) = \left[\hat{f}(x) \pm (\gamma_1 \times \text{aleatoric}(x) + \gamma_2 \times \text{epistemic}(x)) \right], \quad \text{with } \gamma_2 = \lambda \gamma_1, \quad (1)$$

where \hat{f} is a point estimate, and $\gamma_1, \gamma_2 \in [0, \infty)$ are coefficients selected to 1) calibrate marginal coverage and 2) optimally balance the two types of uncertainty (optimality is defined in terms of a quantile loss metric introduced later). The parameter λ controls the trade-off between the two uncertainty types: when $\lambda = 0$, the interval reflects only aleatoric uncertainty, while as $\gamma_1 \rightarrow 0$, $\lambda = \frac{\gamma_2}{\gamma_1} \rightarrow \infty$, it reflects only epistemic uncertainty. By allowing an adaptively chosen λ , we ensure a more flexible and data-driven trade-off to the two components, leading to prediction intervals that are both well-calibrated and more informative (Figure 1). Moreover, estimating λ can help practitioners better understand which source of uncertainty is the dominant contributor to the overall uncertainty.

The combination of epistemic and aleatoric uncertainty is not new: Bayesian methods have long incorporated both components [17, 18], and several recent approaches have also explored this decomposition in the context of conformal prediction [19–21]. However, to the best of our knowledge, existing methods either do not explicitly distinguish between the two types of uncertainty or implicitly fix the combination ratio, for instance, setting $\lambda = 1$ as in [22, 17, 18], or fixing $\gamma_1 = 1$ as in [19]. This fixed choice may be suboptimal, as the relative importance of each uncertainty type varies with the data distribution and prediction task (see Appendix A for more details on related work).

1.1 Contributions

1. We are the first to introduce two calibration parameters γ_1 and γ_2 to balance the scale of epistemic and aleatoric uncertainty on the validation dataset.
2. We demonstrate that fitting quantiles on the residuals provides much more sensible estimators of aleatoric uncertainty than fitting the quantiles directly on the targets.
3. We are the first to combine the ensemble perturbation intervals via PCS framework ([23] and [24, Chapter 13]) with the CQR aleatoric uncertainty estimator, and empirically show the strengths of this combination.
4. We take a step towards large-scale benchmarking of uncertainty quantification by extending the PCS-UQ framework of [23] to methods based on quantile regression.

The remainder of the paper is organized as follows: Section 2 introduces the CLEAR methodology. Section 3 outlines the experimental setup, including synthetic simulations, real-world datasets, baselines, and metrics. Section 4 presents results and a case study of the PCS pipeline. Section 5 concludes with limitations and future directions.

2 Method

2.1 Problem scenario

Consider a classical setting, where an i.i.d. sample $(X_i, Y_i), i = 1, \dots, n$ is drawn from distribution $P_X \times P_{Y|X}$. The goal of conformal inference is to construct a prediction set $C(X_{n+1}) \subseteq \text{supp}(Y)$ for a new data-point (X_{n+1}, Y_{n+1}) satisfying marginal coverage

$$\mathbb{P}(Y_{n+1} \in C(X_{n+1})) \geq 1 - \alpha, \quad (2)$$

where $\alpha \in (0, 1)$ is for example $\alpha = 0.05$. In order to construct C , data $\mathcal{D} = \{(X_i, Y_i), i = 1, \dots, n\}$ can be split into train and calibration subsets $\mathcal{D}_{\text{train}}, \mathcal{D}_{\text{cal}}$. On the training data, a first estimate of C can be constructed, and then we can use data from \mathcal{D}_{cal} to calibrate C such that (2) is satisfied.

In case of CQR, we first estimate conditional quantiles $\hat{q}_{\alpha/2}(x), \hat{q}_{1-\alpha/2}(x)$ using $\mathcal{D}_{\text{train}}$, and then construct $C(x) = [\hat{q}_{\alpha/2}(x) - \gamma, \hat{q}_{1-\alpha/2}(x) + \gamma]$, where the calibration parameter γ is chosen so that the prediction interval $C(X_i)$ contains Y_i for exactly $\lceil (1 - \alpha)(|\mathcal{D}_{\text{cal}}| + 1) \rceil$ points in the calibration set \mathcal{D}_{cal} . While this procedure guarantees finite-sample distribution-free marginal coverage [8], conditional coverage

$$\mathbb{P}(Y_{n+1} \in C(X_{n+1}) \mid X_{n+1} = x) \geq 1 - \alpha$$

does not need to hold. As pointed out in [25, 26], any algorithm with finite-sample distribution-free conditional coverage guarantees for all x must be trivial $C(x) = (-\infty, \infty)$. However, we aim to design estimators such that conditional coverage holds approximately under reasonable real-world scenarios, even if exact finite-sample guarantees are impossible in general.

2.2 Epistemic uncertainty

The traditional machine learning approach trains a predictive algorithm on a single version of the cleaned/preprocessed dataset and uses the best-performing algorithm (compared using the validation set) for future predictions. While theoretically sound in the infinite-sample limit, this approach ignores the uncertainty stemming from finite sample size and model choice (epistemic uncertainty). Various methods have been proposed to estimate this uncertainty, including Deep Ensembles [22], MC dropout in NN [27], Orthonormal Certificates [13], NOMU [28], BNNs [29], Laplace Approximation [30], to name a few.

Estimating Epistemic Uncertainty via PCS: In practice, additional sources of uncertainty arise from subjective choices in data cleaning, imputation, and dataset construction, which we also consider as extended epistemic uncertainty. The Predictability, Computability, and Stability (PCS) framework [24, 23, 31] offers a holistic point of view on the data-science-life-cycle, though it does not explicitly model aleatoric uncertainty. Following [24, Chapter 13], we obtain an ensemble of m estimators $\hat{f}_1, \dots, \hat{f}_m$ as follows:

1. We split the data into $\mathcal{D}_{\text{train}}, \mathcal{D}_{\text{val}}$.
2. We create N_1 differently preprocessed versions of the data and define N_2 different models (such as linear regression, random forest, neural networks, etc.). We train models for all $N_1 \times N_2$ combinations on $\mathcal{D}_{\text{train}}$ and pick the top- k based on their performance on \mathcal{D}_{val} .
3. We refit each of the top- k models on b bootstrap samples $\mathcal{D}_{\text{train}}^1, \dots, \mathcal{D}_{\text{train}}^b$ of $\mathcal{D}_{\text{train}}$ to obtain an ensemble of $m = k \times b$ estimators $\hat{f}_1, \dots, \hat{f}_m$.

Taking the point-wise median of $\hat{f}_1, \dots, \hat{f}_m$, yields the final PCS estimate \hat{f} , and the point-wise $\alpha/2$ and $1 - \alpha/2$ quantiles (denoted $\hat{f}_{\alpha/2}$ and $\hat{f}_{1-\alpha/2}$, respectively) define the (uncalibrated) uncertainty band. The widths of this interval, denoted as $\hat{q}_{1-\alpha/2}^{\text{epi}}(x) := \hat{f}_{1-\alpha/2}(x) - \hat{f}(x)$ and $\hat{q}_{\alpha/2}^{\text{epi}}(x) := \hat{f}(x) - \hat{f}_{\alpha/2}(x)$, quantifies the pre-calibrated epistemic uncertainty.

For implementation details of PCS uncertainty quantification, see Appendix C.2. A recent extension of PCS uncertainty quantification [23] uses the combined data set $\mathcal{D}_{\text{train}} \cup \mathcal{D}_{\text{val}}$ for training and calibrates uncertainty based on out-of-bag data. We expect that CLEAR could benefit from incorporating such refinements. Although most of our experiments only cover the modeling step of the PCS framework, as in [23], in Section 4.3 we also account for uncertainty due to data cleaning and pre-processing on a case study following Chapter 13 in [24].

2.3 Aleatoric uncertainty

Aleatoric uncertainty can be estimated by modeling the conditional distribution of the outcome given the inputs. Common approaches include direct conditional quantile regression [32], either parametric or nonparametric, such as smooth quantile regression [33] and quantile random forests (QRF) [34]; heteroskedastic models that estimate input-dependent noise levels $\sigma(x)$ under Gaussian assumptions [35]; and distributional regression techniques such as simultaneous quantile regression [13]. More flexible alternatives include conditional density estimation and deep generative models such as conditional generative adversarial networks, conditional variational autoencoders, or diffusion models [36–38].

In this work, we estimate aleatoric uncertainty using quantile regression models $\hat{r}_{\alpha/2}, \hat{r}_{0.5}, \hat{r}_{1-\alpha/2}$ (selected in step 2 from PCS) trained on the residuals $Y_i - \hat{f}(X_i)$. This approach offers improved stability: underfitting quantile regression directly on the y -values can severely distort aleatoric uncertainty estimates. In contrast, extreme underfitting on residuals, at worst, corresponds to assuming homoscedastic noise, which can be an acceptable bias. This improves the stability with respect to hyperparameters. To further improve the stability, we apply a PCS-inspired bagging strategy. From the aggregated estimators of $\hat{r}_{\alpha}, \hat{r}_{0.5}, \hat{r}_{1-\alpha}$, we compute $\hat{q}_{1-\alpha/2}^{\text{ale}}(x) := \hat{r}_{1-\alpha/2}(x) - \hat{r}_{0.5}(x)$ and $\hat{q}_{\alpha/2}^{\text{ale}}(x) := \hat{r}_{0.5}(x) - \hat{r}_{\alpha/2}(x)$. Overall, it is computationally efficient and straightforward to implement.

2.4 CLEAR: combining aleatoric & epistemic uncertainty

To combine both aleatoric and epistemic uncertainties, we use a weighted scheme as in Equation (1). Specifically, using a PCS-type estimator $\hat{q}_{\alpha}^{\text{epi}}$ and a quantile regression estimator $\hat{q}_{\alpha}^{\text{ale}}$ trained on the residuals $Y_i - \hat{f}(X_i)$, we define the prediction interval:

$$C = \left[\hat{f} - \gamma_1 \hat{q}_{\alpha/2}^{\text{ale}} - \gamma_2 \hat{q}_{\alpha/2}^{\text{epi}}, \quad \hat{f} + \gamma_1 \hat{q}_{1-\alpha/2}^{\text{ale}} + \gamma_2 \hat{q}_{1-\alpha/2}^{\text{epi}} \right]. \quad (3)$$

Given a fixed ratio $\lambda = \frac{\gamma_2}{\gamma_1}$, we compute γ_1 on a held-out calibration set using the standard split conformal prediction procedure. While the natural choice $\gamma_1 = \gamma_2$ may seem appealing, it is often suboptimal. This is because the relative contribution of aleatoric and epistemic uncertainty can vary across datasets, and the corresponding estimators may differ substantially in scale and precision.

To choose λ from data, we evaluate a grid of positive values Λ . For each candidate $\lambda \in \Lambda$, we construct the (calibrated) interval C_{λ} . To ensure the best trade-off between uncertainty sources, we select λ^* such that C_{λ^*} performs best under the chosen metric on \mathcal{D}_{val} . We have chosen quantile loss [32] (defined in Algorithm 1, also known as pinball loss) as a simple metric to balance both coverage and width. However, any other metric can also be used. As a proper scoring rule, quantile loss incentivizes truthfulness from a theoretical perspective. This procedure is summarized in Algorithm 1.

In the case that either the estimation of epistemic or the estimation of aleatoric uncertainty terribly fails, λ^* can compensate this failure to some extent by giving more weight on the other estimator. In the other (hopefully more likely) case, that both estimators \hat{q}^{epi} and \hat{q}^{ale} perform reasonably well (up to incorrect scaling), λ^* can provide valuable insights beyond predictive inference: A very large value $\lambda^* \frac{\hat{q}_{1-\alpha/2}^{\text{epi}}(x) + \hat{q}_{\alpha/2}^{\text{epi}}(x)}{\hat{q}_{1-\alpha/2}^{\text{ale}}(x) + \hat{q}_{\alpha/2}^{\text{ale}}(x)} \gg 1$ hints that epistemic uncertainty dominates the uncertainty for x , and is expected to reduce if you collect more training observations close to x (or by making stronger and better modeling assumptions). Vice versa, a small value $\lambda^* \frac{\hat{q}_{1-\alpha/2}^{\text{epi}}(x) + \hat{q}_{\alpha/2}^{\text{epi}}(x)}{\hat{q}_{1-\alpha/2}^{\text{ale}}(x) + \hat{q}_{\alpha/2}^{\text{ale}}(x)} \ll 1$ hints that aleatoric uncertainty dominates for x which cannot be reduced by collecting more training observations. In some cases, the aleatoric uncertainty can be reduced by changing the problem formulation by increasing the dimension of x (i.e., by measuring more co-variables for the training and validation dataset and for the new datapoint x).

Lemma 2.1. *Let Λ be compact. Suppose that at least k of the base models used in the PCS ensemble are consistent for the true function $f(x)$, and the quantile regression estimators $\hat{q}_{\tau}^{\text{ale}}$ are consistent for both $\tau \in \{\alpha/2, 1 - \alpha/2\}$. Then we obtain **asymptotic conditional validity**: for any fixed $x \in \mathcal{X}$, it holds that*

$$\liminf_{|\mathcal{D}_{\text{train}}|, |\mathcal{D}_{\text{cal}}| \rightarrow \infty} \mathbb{P}(Y_{n+1} \in C(X_{n+1}) \mid X_{n+1} = x) \geq 1 - \alpha.$$

Algorithm 1 CLEAR: Calibrated Learning for Epistemic and Aleatoric Risk

1: **Input:** Data (X_i, Y_i) for $i = 1, \dots, n$, split into training $\mathcal{D}_{\text{train}}$, calibration \mathcal{D}_{cal} , and validation \mathcal{D}_{val} (we consider $\mathcal{D}_{\text{cal}} = \mathcal{D}_{\text{val}}$); grid of λ values Λ ; significance level α .

2: **Step 1: Estimate epistemic uncertainty on $\mathcal{D}_{\text{train}}$.**

Example: Estimate stable point predictor \hat{f} and epistemic quantiles $\hat{q}_{\alpha/2}^{\text{epi}}, \hat{q}_{1-\alpha/2}^{\text{epi}}$ using PCS ensembles across data perturbations.

3: **Step 2: Estimate aleatoric uncertainty on $\mathcal{D}_{\text{train}}$.**

Example: train a quantile regression model on the residuals $Y_i - \hat{f}(X_i)$ to estimate conditional quantiles $\hat{q}_{\alpha/2}^{\text{ale}}, \hat{q}_{1-\alpha/2}^{\text{ale}}$.

4: **Step 3: Define prediction intervals for each $\lambda \in \Lambda$.**

Define C_λ by selecting the smallest value γ_1 such that the prediction set

$$C_\lambda = \left[\hat{f} - \gamma_1 \hat{q}_{\alpha/2}^{\text{ale}} - \lambda \gamma_1 \hat{q}_{\alpha/2}^{\text{epi}}, \hat{f} + \gamma_1 \hat{q}_{1-\alpha/2}^{\text{ale}} + \lambda \gamma_1 \hat{q}_{1-\alpha/2}^{\text{epi}} \right]$$

contains at least $\lceil (1 - \alpha)(|\mathcal{D}_{\text{cal}}| + 1) \rceil$ of points in \mathcal{D}_{cal} . See Appendix B for a detailed implementation.

5: **Step 4: Select λ^* that minimizes a chosen evaluation metric.**

For any metric in Appendix C.3 (e.g., quantile loss), evaluate $C_\lambda(x)$ on \mathcal{D}_{val} and set

$$\lambda^* = \arg \min_{\lambda \in \Lambda} \text{QuantileLoss}(\mathcal{D}_{\text{val}}, C_\lambda),$$

where $\text{QuantileLoss}(\mathcal{D}_{\text{val}}, C_\lambda) := \sum_{i \in \mathcal{D}_{\text{val}}} [QL_{\alpha/2}(Y_i, l(X_i)) + QL_{1-\alpha/2}(Y_i, u(X_i))] / 2$, with $l(x), u(x)$ denoting the bounds of $C_\lambda(x)$, and $QL_\tau(y, q) = (y - q)(\tau - \mathbb{1}_{(-\infty, q]}(y))$.

6: **Output:** λ^* and calibrated prediction interval $C_{\lambda^*}(x)$.

Proof. The consistency of the predictors implies $\hat{q}_\tau^{\text{epi}}(x) \rightarrow 0$, and the consistency of the quantile estimators implies $\hat{q}_\tau^{\text{ale}}(x) \rightarrow q_\tau^{\text{ale}}(x)$ point-wise. Hence, the estimated pre-calibrated intervals converge to their population analogues. Since $\sup_{\lambda \in \Lambda} \lambda \hat{q}_\tau^{\text{epi}}(x) \rightarrow 0$ converges to 0 uniformly over $\lambda \in \Lambda$ (due to compactness of Λ), therefore $C(x)$ is asymptotically equal to true conditional quantiles $[r_{\alpha/2}(x), r_{1-\alpha/2}(x)]$; and necessarily $\lim_{|\mathcal{D}_{\text{cal}}| \rightarrow \infty} \gamma_1 = 1$, as is the case in classical CQR (see e.g. [8, Section 5]). \square

Note that these assumptions are satisfied by the finite grid Λ used in our implementation and by many base models, including tree-based methods and neural networks. We elaborate on the theoretical implications in Appendix G, where formal guarantees for marginal coverage are provided in Lemma G.2.

3 Experimental Setup

3.1 Simulations

We conduct simulations on synthetic data to assess the theoretical guarantees of our approach. We sampled $X \sim \mathcal{N}(0_d, I_d)$ and computed the response $Y = \mu(X) + \sigma(X) \cdot \varepsilon$, where $\varepsilon \sim \mathcal{N}(0, 1)$. The mean function $\mu(X)$ introduced non-linearity through transformations of input features (involving absolute values and fractional powers with random coefficients); its explicit form, alongside $\sigma(X)$, is detailed in Appendix D. The sample size was fixed at $n = 5000$ and divided into 70-30% training and validation splits. In the univariate case, we generate 100 datasets for $d = 1$, and in multivariate, 100 datasets randomly sampled for $d \in \{2, 3, 20\}$. We then assess the conditional performance as a function of distance from the training data, where test points are randomly generated on the surfaces of spheres with varying radii (see Appendix D for full explanation).

3.2 Datasets

To evaluate our method in real-world scenarios, we apply it to 17 publicly available regression datasets curated by [23, 39], forming one of the largest benchmarks of its kind and spanning diverse

domains such as housing, energy, materials science, and healthcare [40–58]. Categorical features are one-hot encoded, with no further preprocessing. To ensure robustness, each dataset is evaluated over 10 random train-validation-test splits (60%-20%-20%). Note that we use our validation set \mathcal{D}_{val} also as calibration set \mathcal{D}_{cal} throughout this paper. A summary of the datasets is provided in Appendix E.

3.3 Baselines

We compare CLEAR against its core components, CQR and PCS ensemble (we also explore other baselines defined in Appendix C.1, which we only present in the appendices). Notably, the underlying uncertainty estimation models from CQR and PCS are reused within the CLEAR framework. Our CQR follows classical implementation [9] with the difference that in our experiments, we primarily utilize an enhanced variant, termed **ALEATORIC**, which uses bootstrapping ($b = 100$) on Y_i and the model selection from PCS. We further improve ALEATORIC in a new baseline called **ALEATORIC-R**, which models the residuals $Y_i - \hat{f}(X_i)$ instead, using \hat{f} from the corresponding PCS ensemble. The CLEAR method presented uses the uncalibrated aleatoric uncertainty estimate from this ALEATORIC-R and the uncalibrated epistemic uncertainty from PCS. For fairness and cross-comparison, the model type for quantile estimation within the ALEATORIC-R model is determined by the best-chosen model for epistemic uncertainty.

We perform ablation studies by exploring three different variants of base models for PCS (epistemic) and CQR (aleatoric). Our main approach, which we refer to as **variant (a)**, uses a **quantile PCS** for estimating epistemic uncertainty. We employ a diverse set of models designed to estimate conditional quantiles, namely quantile random forests (QRF) [34], quantile XGBoost (QXGB) [59], and Expectile GAM [60]. Then, the top-performing model ($k = 1$) on the validation set is selected and bootstrapped ($b = 100$) to generate the epistemic uncertainty estimate \hat{q}^{epi} and the median \hat{f} . CLEAR then combines this bootstrapped \hat{q}^{epi} with the bootstrapped aleatoric estimate from ALEATORIC-R, ensuring ALEATORIC-R also uses the same selected quantile model. The other two variants are explained in Appendix C.2, both using the same b and k as above and only modifying the models. **Variant (b)** restricts quantile PCS as well as CQR baselines to **only QXGB** to remove any impact on CLEAR’s evaluation due to the choice of the base models. In contrast, **variant (c)** uses the standard PCS models from [24, 23] to estimate the **conditional mean**. In all cases, PCS intervals are calibrated using the multiplicative method.

CLEAR parameters (λ, γ_1) are optimized via quantile loss on the validation set. λ is chosen from a dense grid combining linearly spaced values from 0 to 0.09 and logarithmically spaced values from 0.1 to 100 (totaling over 4000 points), and γ_1 is determined via conformal calibration for the chosen λ . All intervals are evaluated at 95% nominal coverage. In our benchmarks, we only tackle the model perturbations of PCS and not the data processing part, where we simplify the process to a single dataset (i.e., $N_1 = 1$) as in [23]. However, we show an example in Section 4.3 of how CLEAR can be applied in the $N_1 > 1$ setting from [24, Chapter 13].

3.4 Metrics

To evaluate the quality of our prediction intervals, we employ interval coverage (PICP), normalized interval width (NIW), average interval score loss and the quantile loss that are common in the interval prediction literature [61–64]. We also evaluate our work on Normalized Calibrated Interval Width (NCIW), defined as:

$$\text{NCIW}(\hat{f}, l, u) = \text{NIW} \left(\hat{f} - c_{\text{test-cal}} l, \hat{f} + c_{\text{test-cal}} u \right),$$

with a calibration constant

$$c_{\text{test-cal}} := \arg \min_{c \geq 0} \left\{ \text{PICP} \left(\hat{f} - cl, \hat{f} + cu \right) \geq 1 - \alpha \right\}.$$

Since we only compare methods that were already calibrated on the validation dataset, they all approximately have the correct coverage on the test set, resulting in $c_{\text{test-cal}} \approx 1$. Detailed definitions and closed-form expressions for these metrics are given in Appendix C.3. We primarily discuss NCIW and quantile loss, but provide the results for all the available metrics.

4 Results

4.1 Simulations

Figure 2 shows conditional coverage and interval width for the univariate homoskedastic case. While ALEATORIC-R achieve good coverage in high-density regions but under-cover in low-density or extrapolation regions. When aleatoric and epistemic uncertainties are correlated, all methods perform similarly in the data-rich region, but only CLEAR maintains correct conditional coverage throughout, adapting interval width as needed. Additional results for heteroskedastic and multivariate settings in Appendix D show similar findings.

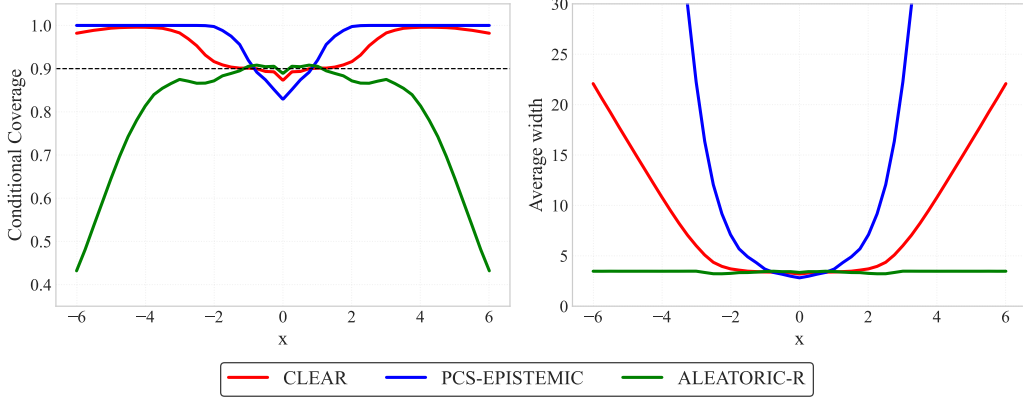


Figure 2: Results for univariate homoskedastic case averaged over 100 simulations: On the left, conditional coverage, and on the right, mean width, for $X = x$. The plot compares CLEAR, PCS, and ALEATORIC-R (CQR with bootstrapping and trained on residuals $Y_i - \hat{f}(X_i)$). The dashed horizontal line represents the target coverage level of 0.9. CLEAR adapts to maintain target coverage across the input space.

4.2 Real-world data

Figure 3 shows the Normalized Calibrated Interval Width (NCIW) and Quantile Loss for 95% prediction intervals across all datasets for our main configuration, CLEAR (variant a), compared to several baselines. CLEAR consistently demonstrates superior performance, achieving better or comparable interval width and loss metrics while rigorously maintaining nominal coverage.

The inset boxplots in Figure 3 quantitatively illustrate this advantage: compared to CLEAR (a), PCS, ALEATORIC, and ALEATORIC-R show increases in quantile loss of 15.8%, 34.5%, and 9.4%, respectively. Similar relative increases are observed for NCIW, with PCS, ALEATORIC, and ALEATORIC-R exhibiting increases of 17.4%, 28.2%, and 3%. Moreover, CLEAR (a) was in fact the top-performing method on 15 of the 17 datasets while it stayed the most stable compared to the baselines. These trends hold across our other model variants as well (Appendix E for full results): both CLEAR (b) and CLEAR (c) exhibit very similar relative improvements (Figures 7 and 8 in Appendices E.2 and E.3), with variant (a) remaining the strongest and most robust configuration.

While we observed that setting $\lambda = 1$ or $\gamma_1 = 1$ could marginally improve results if one had prior knowledge of uncertainty components—an unlikely scenario in practice—fully optimizing both parameters offers greater robustness. A limited size of the validation dataset can lead to overfitting of the two parameters. Incorporating some prior on these 2 parameters could potentially further improve CLEAR results. Importantly, the absolute value of λ is relative to the pre-calibrated scales of the uncertainty estimators and dataset noise; its interpretation is best contextualized by observing its behavior when systematically varying dataset characteristics, such as the number of features or observations.

Although the reliability of the prediction intervals is critical, we noticed that stand-alone baselines, including ALEATORIC and PCS ensembles, can occasionally exhibit instability on certain datasets, potentially resulting in overly wide or miscalibrated prediction intervals. This characteristic is ev-

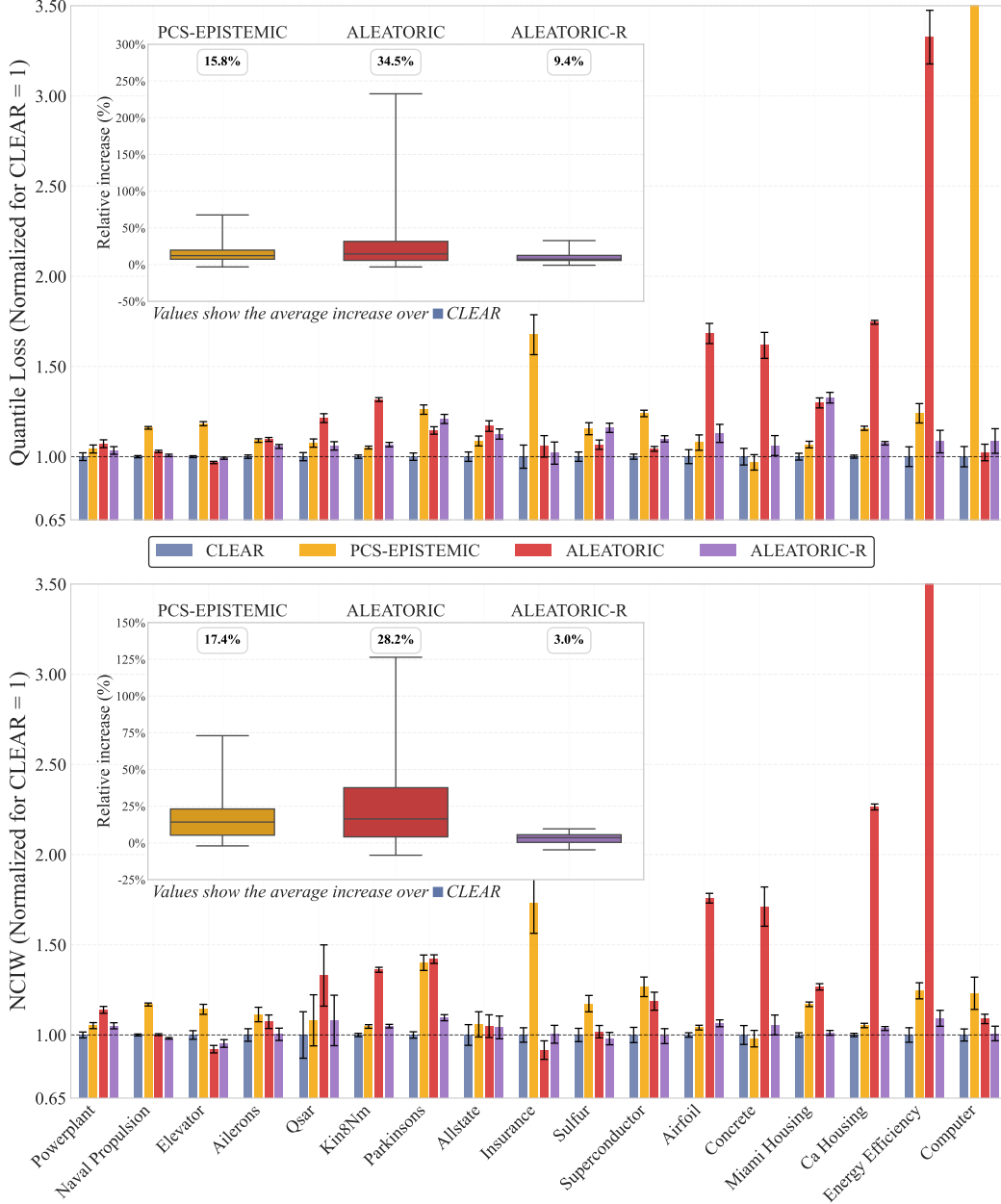


Figure 3: Results for real-world data: Quantile loss and NCIW performance of different methods over 10 seeds normalized relative to CLEAR (baseline = 1.0). Lower values indicate better performance. Error bars represent ± 1 standard deviation across seeds. The inset boxplot shows the % of the relative increase of the metric over CLEAR aggregated over all datasets, with the printed numbers displaying an average increase. EPISTEMIC is using the PCS-UQ framework [23]. ALEATORIC is an improved CQR (PCS-inspired with bootstrapping according to [24, Chapter 13]). ALEATORIC-R is further improved by our residual approach. All methods use \hat{f} from PCS.

ident in instances such as the energy_efficiency dataset (Table 9), where ALEATORIC shows a markedly larger NCIW compared to CLEAR. In contrast, CLEAR’s residual modeling and dual-parameter calibration mechanism enhance stability by adaptively re-weighting potentially unreliable or mis-scaled uncertainty components, particularly epistemic estimates; CLEAR consistently produces sharper and more reliable intervals. The extensive dataset-dependent variability observed in the optimal λ further highlights the necessity of CLEAR’s adaptive λ selection over fixed heuristics, enabling performance that is optimally tailored to the specific characteristics of each dataset.

4.3 Case study: Complete PCS framework

We consider a case study on the Ames Housing dataset, detailed in Appendix F, where (1) we demonstrate the full PCS pipeline, capturing uncertainty from both data preprocessing and model evaluation and (2) we vary the number of predictor variables used to model housing prices. Starting from approximately 80 features, we construct a reduced version using only the top two predictors based on feature importance; this setup naturally balances between aleatoric uncertainty (increases due to limited information) and epistemic uncertainty (decreases due to reduced model complexity). Table 1 reveals that while PCS performs better with many predictors and CQR excels with fewer features, CLEAR adapts effectively to both scenarios through its calibrated uncertainty combination. CLEAR estimates $\lambda = 0.6$ in the 2-variable case (prioritizing aleatoric uncertainty) versus $\lambda = 14.5$ in the full-feature case (emphasizing epistemic uncertainty), with corresponding epistemic-to-aleatoric ratios of 0.03 and 7.72. This adaptive weighting enables CLEAR to maintain sharp and well-calibrated intervals across both scenarios, evidenced by the nearly halved average interval width when using all features; suggesting that adding covariates effectively reduces uncertainty.

Table 1: Ames Housing results (90% coverage target).

Experiment	Method	Coverage	Average Width (\$)	Quantile Loss	NCIW
2 features	PCS	0.87	107,880	3,818	0.213
	CQR	0.89	104,741	3,448	0.186
	CLEAR	0.89	98,571	3,191	0.179
All features	PCS	0.89	57,594	1,922	0.105
	CQR	0.87	62,398	2,194	0.117
	CLEAR	0.89	56,745	1,873	0.102

5 Conclusion, Limitations & Future Work

This paper introduces CLEAR, a novel framework for constructing prediction intervals by adaptively balancing epistemic and aleatoric uncertainty. Through a calibration process involving two distinct parameters, γ_1 and γ_2 , CLEAR offers an improvement over conventional methods that often address these uncertainty types in isolation or rely on their fixed, non-adaptive combination. Our evaluations using CQR for aleatoric uncertainty and PCS for epistemic uncertainty show that interval width and quantile loss improve on both simulated and the 17 real-world datasets. The method consistently achieves improved conditional coverage, notably by adapting interval widths appropriately in extrapolation regions, and yields narrower average interval widths compared to a suite of strong baseline methods, thereby providing more precise and reliable uncertainty estimates.

Limitations remain despite CLEAR’s significant advantages and these warrant further discussion. From a practical standpoint, the computational overhead associated with our method involves training an ensemble for epistemic uncertainty and fitting models for aleatoric uncertainty. We must note that bootstrapping for the aleatoric part is not necessary; however, the reliance on ensemble techniques and bootstrapping for epistemic uncertainty estimation, while effective, can face scalability challenges with large datasets or models. The accuracy of CLEAR is intrinsically linked to the quality of the base estimators for epistemic and aleatoric uncertainty, with its re-weighting being sensitive to the size and representativeness of the calibration set. Epistemic uncertainty, as shown in the case study, must be handled using careful judgment calls, in line with the principles of the PCS framework [31, 24]. The additive combination of scaled uncertainties, while powerful, is also a specific structural choice.

Future work could explore several promising directions. A natural modification of the CLEAR framework is its extension to classification tasks, where disentangled uncertainty estimates may also improve calibration [65]. Additionally, investigating better techniques for choosing the λ parameter beyond the performance on a validation set might refine its selection process. Another direction is integrating CLEAR with active learning paradigms, where its uncertainty decomposition could guide more efficient data acquisition [15]. Moreover, exploring alternative, potentially more scalable, approaches for epistemic uncertainty quantification, such as those based on Vine Copulas [66] or other non-ensemble methods, could mitigate current computational limitations and ease the framework’s adoption. Extending CLEAR to time series settings could also be valuable, especially for capturing temporal uncertainty dynamics [67–75]. Finally, a deeper study into the interpretability of the learned λ and γ_1 parameters could provide insights into the dominant sources of uncertainty in various contexts.

Acknowledgments and Disclosure of Funding

We are grateful to Abhineet Agarwal and Michael Xiao for their valuable feedback, helpful discussions, and for sharing early previews and detailed explanations of their code. We also thank Natasa Tagasovska, Jakob Weissteiner, Hanna Wutte, Florian Krach, Markus Chardonnet, Josef Teichmann, Bertrand Charpentier, Janis Postels, Alexander Immer, Erez Buchweitz, João Vitor Romano, Omer Ronen, James-A. Goulet, and Hans Bühler for insightful and stimulating discussions. We are also grateful to Valérie Chavez-Demoulin for her continuous support.

Juraj Bodik acknowledges support from the Hasler Foundation [grant number 24009]. Part of this work was conducted during his research visit to the UC Berkeley, supported by the Hasler Foundation. He thanks the Department of Statistics at UC Berkeley for their kind hospitality.

Jakob Heiss acknowledges support from the Swiss National Science Foundation (SNSF) Postdoc.Mobility fellowship [grant number P500PT_225356]. Early ideas for this work began to take shape while he was affiliated with the Department of Mathematics, ETH Zürich, Switzerland.

We gratefully acknowledge partial support from NSF grant DMS-2413265, NSF grant DMS 2209975, NSF grant 2023505 on Collaborative Research: Foundations of Data Science Institute (FODSI), the NSF and the Simons Foundation for the Collaboration on the Theoretical Foundations of Deep Learning through awards DMS-2031883 and 814639, NSF grant MC2378 to the Institute for Artificial CyberThreat Intelligence and Operation (ACTION), and NIH (DMS/NIGMS) grant R01GM152718.

References

- [1] M. Abdar, F. Pourpanah, S. Hussain, D. Rezazadegan, L. Liu, M. Ghavamzadeh, P. Fieguth, X. Cao, A. Khosravi, U. R. Acharya, V. Makarenekov, and S. Nahavandi. A review of uncertainty quantification in deep learning: Techniques, applications and challenges. *Information Fusion*, 76:243–297, 2021.
- [2] J. Gawlikowski, C. R. N. Tassi, M. Ali, and et.al. A survey of uncertainty in deep neural networks. *Artificial Intelligence Review*, 56(1):1513–1589, 2023.
- [3] V. Kuleshov, N. Fenner, and S. Ermon. Accurate uncertainties for deep learning using calibrated regression. In *Proceedings of the 35th International Conference on Machine Learning*, volume 80 of *Proceedings of Machine Learning Research*, pages 2796–2804. PMLR, 10–15 Jul 2018.
- [4] V. Vovk, A. Gammerman, and G. Shafer. *Algorithmic Learning in a Random World*. Springer Science & Business Media, 2005.
- [5] V. Vovk, I. Nouretdinov, and A. Gammerman. On-line predictive linear regression. *The Annals of Statistics*, 37(3):1566–1590, 2009.
- [6] V. Vovk. Conditional validity of inductive conformal predictors. In *Asian Conference on Machine Learning*, pages 475–490, 2012.
- [7] V. Vovk. Transductive conformal predictors. In *IFIP International Conference on Artificial Intelligence Applications and Innovations*, pages 348–360. Springer, 2013.
- [8] A. N. Angelopoulos, R. F. Barber, and S. Bates. Theoretical foundations of conformal prediction, 2024.
- [9] Y. Romano, E. Patterson, and E. Candès. Conformalized quantile regression. In *Advances in Neural Information Processing Systems*, volume 32. Curran Associates, Inc., 2019.
- [10] I. Gibbs, J. J. Cherian, and E. J. Candès. Conformal prediction with conditional guarantees, 2024.
- [11] E. Hüllermeier and W. Waegeman. Aleatoric and epistemic uncertainty in machine learning: an introduction to concepts and methods. *Machine Learning*, 110:457–506, 2021.

- [12] M. Kirchhof, G. Kasneci, and E. Kasneci. Reexamining the aleatoric and epistemic uncertainty dichotomy. In *ICLR Blogposts 2025*, 2025. <https://iclr-blogposts.github.io/2025/blog/reexamining-the-aleatoric-and-epistemic-uncertainty-dichotomy/>.
- [13] N. Tagasovska and D. Lopez-Paz. Single-model uncertainties for deep learning. In *Advances in Neural Information Processing Systems*, volume 32. Curran Associates, Inc., 2019.
- [14] M. Laves, S. Ihler, J. F. Fast, L. A. Kahrs, and T. Ortmaier. Recalibration of aleatoric and epistemic regression uncertainty in medical imaging. *Machine Learning for Biomedical Imaging*, 1:1–26, 2021.
- [15] B. Settles. *Active Learning*, volume 1 of *Synthesis Lectures on Artificial Intelligence and Machine Learning*. Springer Cham, 1 edition, 2012. Synthesis Collection of Technology (R0), eBColl Synthesis Collection 4.
- [16] L. Marques and D. Berenson. Quantifying aleatoric and epistemic dynamics uncertainty via local conformal calibration, 2024.
- [17] A. Kendall and Y. Gal. What uncertainties do we need in bayesian deep learning for computer vision?, 2017.
- [18] S. Depeweg, J. Hernandez-Lobato, F. Doshi-Velez, and S. Udluft. Decomposition of uncertainty in Bayesian deep learning for efficient and risk-sensitive learning. In *Proceedings of the 35th International Conference on Machine Learning*, volume 80 of *Proceedings of Machine Learning Research*, pages 1184–1193. PMLR, 10–15 Jul 2018.
- [19] R. Rossellini, R. Barber, and R. Willett. Integrating uncertainty awareness into conformalized quantile regression, 2024.
- [20] L. M. C. Cabezas, V. S. Santos, T. R. Ramos, and R. Izbicki. Epistemic uncertainty in conformal scores: A unified approach, 2025.
- [21] P. Hofman, Y. Sale, and E. Hüllermeier. Quantifying aleatoric and epistemic uncertainty with proper scoring rules, 2024.
- [22] B. Lakshminarayanan, A. Pritzel, and C. Blundell. Simple and scalable predictive uncertainty estimation using deep ensembles. In *Advances in Neural Information Processing Systems*, volume 30. Curran Associates, Inc., 2017.
- [23] A. Agarwal, M. Xiao, R. Barter, O. Ronen, B. Fan, and B. Yu. Pcs-uv: Uncertainty quantification via the predictability-computability-stability framework. *arXiv preprint arXiv:2505.08784*, 2025.
- [24] B. Yu and R. L. Barter. *Veridical Data Science: The Practice of Responsible Data Analysis and Decision Making*. Adaptive Computation and Machine Learning Series. MIT Press, 2024.
- [25] J. Lei and L. Wasserman. Distribution-free prediction bands for non-parametric regression. *Journal of the Royal Statistical Society: Series B (Statistical Methodology)*, 76, 2014.
- [26] R. F. Barber, E. J. Candès, A. Ramdas, and R. J. Tibshirani. The limits of distribution-free conditional predictive inference, 2020.
- [27] Y. Gal and Z. Ghahramani. Dropout as a bayesian approximation: Representing model uncertainty in deep learning. In *Proceedings of The 33rd International Conference on Machine Learning*, volume 48 of *Proceedings of Machine Learning Research*, pages 1050–1059, New York, New York, USA, 20–22 Jun 2016. PMLR.
- [28] J. M. Heiss, J. Weissteiner, H. S. Wutte, S. Seuken, and J. Teichmann. NOMU: Neural optimization-based model uncertainty. In *Proceedings of the 39th International Conference on Machine Learning*, volume 162 of *Proceedings of Machine Learning Research*, pages 8708–8758. PMLR, 17–23 Jul 2022.
- [29] D. J. C. MacKay. A practical bayesian framework for backpropagation networks. *Neural Computation*, 4(3):448–472, 05 1992.

- [30] H. Ritter, A. Botev, and D. Barber. A scalable laplace approximation for neural networks. In *6th International Conference on Learning Representations (ICLR)*, 2018. Conference Track Proceedings.
- [31] B. Yu and K. Kumbier. Veridical data science. *Proceedings of the National Academy of Sciences*, 117(8):3920–3929, 2020.
- [32] Roger Koenker and Gilbert Bassett. Regression quantiles. *Econometrica*, 46(1):33–50, 1978.
- [33] M. Fasiolo, S. N. Wood, M. Zaffran, R. Nedellec, and Y. Goude. Fast calibrated additive quantile regression. *Journal of the American Statistical Association*, 115(531):1402–1412, 2020.
- [34] N. Meinshausen. Quantile regression forests. *Journal of Machine Learning Research*, 7(35):983–999, 2006.
- [35] D.A. Nix and A.S. Weigend. Estimating the mean and variance of the target probability distribution. In *Proceedings of 1994 IEEE International Conference on Neural Networks (ICNN'94)*, volume 1, pages 55–60 vol.1, 1994.
- [36] P. Oberdiek, G. Fink, and M. Rottmann. Uqgan: A unified model for uncertainty quantification of deep classifiers trained via conditional gans. In *Advances in Neural Information Processing Systems*, volume 35, pages 12345–12356, 2022.
- [37] L. Han, R. Gao, M. Kim, X. Tao, B. Liu, and D. Metaxas. Evidential sparsification of multimodal latent spaces in conditional vaes. In *Advances in Neural Information Processing Systems*, volume 33, pages 14513–14524, 2020.
- [38] Z. Chang, G. A. Koulteris, and H. P. H. Shum. On the design fundamentals of diffusion models: A survey, 2023.
- [39] A. Agarwal and M. Xiao. PCS_UQ: Uncertainty quantification via the predictability, computability, stability (PCS) framework. https://github.com/aagarwal1996/PCS_UQ, 2025. GitHub repository.
- [40] R. Kelley Pace and Ronald Barry. Sparse spatial autoregressions. *Statistics & Probability Letters*, 33(3):291–297, 1997.
- [41] Kaggle. Miami housing dataset. <https://www.kaggle.com/datasets/deepcontractor/miami-housing-dataset>, 2022. Accessed: 2025-04-15.
- [42] P. Tüfekci. Prediction of full load electrical power output of a base load operated combined cycle power plant using machine learning methods. *International Journal of Electrical Power & Energy Systems*, 60:126–140, 2014.
- [43] A. Tsanas and A. Xifara. Accurate quantitative estimation of energy performance of residential buildings using statistical machine learning tools. *Energy and Buildings*, 49:560–567, 2012.
- [44] K. Hamidieh. A data-driven statistical model for predicting the critical temperature of a superconductor. *Computational Materials Science*, 154:346–354, 2018.
- [45] R. Camacho and L. Torgo. Ailerons. <https://www.openml.org/d/296>, 2014. Accessed: 2025-04-15.
- [46] A. Tsanas, M. A. Little, P. E. McSharry, and L. O. Ramig. Accurate telemonitoring of parkinson’s disease progression by noninvasive speech tests. *IEEE Transactions on Biomedical Engineering*, 57:884–893, 2009.
- [47] A. Coraddu, L. Oneto, A. Ghio, S. Savio, D. Anguita, and M. Figari. Machine learning approaches for improving condition-based maintenance of naval propulsion plants. *Proceedings of the Institution of Mechanical Engineers, Part M*, 230(1):136–153, 2016.
- [48] I. Yeh. Modeling of strength of high-performance concrete using artificial neural networks. *Cement and Concrete Research*, 28(12):1797–1808, 1998.

- [49] M. Cassotti, D. Ballabio, R. Todeschini, and V. Consonni. A similarity-based qsar model for predicting acute toxicity towards the fathead minnow (*pimephales promelas*). *SAR and QSAR in Environmental Research*, 26(3):217–243, 2015.
- [50] T. F. Brooks, D. S. Pope, and M. A. Marcolini. Airfoil self-noise and prediction. *NASA Reference Publication*, 1218, 1989.
- [51] PyCaret. Insurance dataset, n.d. Accessed: 2025-04-15.
- [52] L. Torgo. Elevators. <https://www.openml.org/d/216>, 2014. Accessed: 2025-04-15.
- [53] Computer activity. <https://www.openml.org/d/197>, 2014. Accessed: 2025-04-15.
- [54] Allstate claims severity. <https://www.openml.org/d/42571>, 2020. Accessed: 2025-04-15.
- [55] L. Grinsztajn, E. Oyallon, and G. Varoquaux. Why do tree-based models still outperform deep learning on typical tabular data? *Advances in Neural Information Processing Systems*, 35:507–520, 2022.
- [56] Z. Ghahramani. kin8nm dataset, 1996. Accessed: 2025-04-15.
- [57] kin8nm dataset. <https://www.openml.org/d/189>, 2014. Accessed: 2025-04-15.
- [58] sulfur dataset. <https://www.openml.org/d/23515>, 2014. Accessed: 2025-04-15.
- [59] T. Chen and C. Guestrin. XGBoost: A scalable tree boosting system. In *Proceedings of the 22nd ACM SIGKDD International Conference on Knowledge Discovery and Data Mining*, KDD ’16, pages 785–794, New York, NY, USA, 2016. ACM.
- [60] D. Servén and C. Brummitt. pygam: Generalized additive models in python, March 2018.
- [61] T. Gneiting and A. E Raftery. Strictly proper scoring rules, prediction, and estimation. *Journal of the American statistical Association*, 102(477):359–378, 2007.
- [62] T. Pearce, A. Brintrup, M. Zaki, and A. Neely. High-quality prediction intervals for deep learning: A distribution-free, ensembled approach. In *International conference on machine learning*, pages 4075–4084. PMLR, 2018.
- [63] V. V`yugin and V. G. Trunov. Online learning with continuous ranked probability score. In *Proceedings of the Eighth Symposium on Conformal and Probabilistic Prediction and Applications*, volume 105 of *Proceedings of Machine Learning Research*, pages 163–177. PMLR, 09–11 Sep 2019.
- [64] I. Azizi, M. Boldi, and V. Chavez-Demoulin. Semf: Supervised expectation-maximization framework for predicting intervals. *arXiv preprint arXiv:2405.18176*, 2024.
- [65] Y. Romano, M. Sesia, and E. Candès. Classification with valid and adaptive coverage. In *Advances in Neural Information Processing Systems*, volume 33, pages 3581–3591. Curran Associates, Inc., 2020.
- [66] N. Tagasovska, F. Ozdemir, and A. Brando. Retrospective uncertainties for deep models using vine copulas. In *Proceedings of The 26th International Conference on Artificial Intelligence and Statistics*, volume 206 of *Proceedings of Machine Learning Research*, pages 7528–7539. PMLR, 25–27 Apr 2023.
- [67] C. Xu and Y. Xie. Conformal prediction interval for dynamic time-series. In *Proceedings of the 38th International Conference on Machine Learning*, volume 139 of *Proceedings of Machine Learning Research*, pages 11559–11569. PMLR, 18–24 Jul 2021.
- [68] J. Bodik, M. Paluš, and Z. Pawlas. Causality in extremes of time series. *Extremes*, 27:67–121, 2024.
- [69] J. Bodik and O. C. Pasche. Granger causality in extremes, 2024.

- [70] Calypso Herrera, Florian Krach, and Josef Teichmann. Neural jump ordinary differential equations: Consistent continuous-time prediction and filtering. In *International Conference on Learning Representations*, 2021.
- [71] Florian Krach, Marc Nübel, and Josef Teichmann. Optimal estimation of generic dynamics by path-dependent neural jump ODEs. *arXiv preprint arXiv:2206.14284*, 2022.
- [72] William Andersson, Jakob Heiss, Florian Krach, and Josef Teichmann. Extending path-dependent NJ-ODEs to noisy observations and a dependent observation framework. *arXiv*, 2023.
- [73] Florian Krach and Josef Teichmann. Learning Chaotic Systems and Long-Term Predictions with Neural Jump ODEs, July 2024.
- [74] Jakob Heiss, Florian Krach, Thorsten Schmidt, and Félix B. Tambe-Ndonfack. Nonparametric filtering, estimation and classification using neural jump odes, 2024.
- [75] Florian Krach. *Neural Jump Ordinary Differential Equations*. Doctoral thesis, ETH Zurich, Zurich, 2025.
- [76] Ziyu Wang, Tongzheng Ren, Jun Zhu, and Bo Zhang. Function space particle optimization for bayesian neural networks. In *International Conference on Learning Representations*, 2019.
- [77] Florian Wenzel, Jasper Snoek, Dustin Tran, and Rodolphe Jenatton. Hyperparameter ensembles for robustness and uncertainty quantification. In *Proceedings of the 34th International Conference on Neural Information Processing Systems*, NIPS’20, Red Hook, NY, USA, 2020. Curran Associates Inc.
- [78] Yeming Wen, Dustin Tran, and Jimmy Ba. Batchensemble: An alternative approach to efficient ensemble and lifelong learning, 2020.
- [79] Marton Havasi, Rodolphe Jenatton, Stanislav Fort, Jeremiah Zhe Liu, Jasper Snoek, Balaji Lakshminarayanan, Andrew Mingbo Dai, and Dustin Tran. Training independent subnetworks for robust prediction. In *International Conference on Learning Representations*, 2021.
- [80] M. Valdenegro-Toro and D. Saromo. A deeper look into aleatoric and epistemic uncertainty disentanglement, 2022.
- [81] R. C. Edward. Gaussian processes in machine learning. In *Summer school on machine learning*, pages 63–71. Springer, 2003.
- [82] Radford M. Neal. *Bayesian Learning for Neural Networks*, volume 118 of *Lecture Notes in Statistics*. Springer New York, New York, NY, 1996.
- [83] Alex Graves. Practical variational inference for neural networks. In *Advances in neural information processing systems*, pages 2348–2356, 2011.
- [84] Charles Blundell, Julien Cornebise, Koray Kavukcuoglu, and Daan Wierstra. Weight uncertainty in neural networks. In *32nd International Conference on Machine Learning (ICML)*, 2015.
- [85] José Miguel Hernández-Lobato and Ryan Adams. Probabilistic backpropagation for scalable learning of bayesian neural networks. In *International Conference on Machine Learning*, pages 1861–1869, 2015.
- [86] Erik Daxberger, Agustinus Kristiadi, Alexander Immer, Runa Eschenhagen, Matthias Bauer, and Philipp Hennig. Laplace redux - effortless bayesian deep learning. In M. Ranzato, A. Beygelzimer, Y. Dauphin, P.S. Liang, and J. Wortman Vaughan, editors, *Advances in Neural Information Processing Systems*, volume 34, pages 20089–20103. Curran Associates, Inc., 2021.
- [87] Florian Wenzel, Kevin Roth, Bastiaan Veeling, Jakub Swiatkowski, Linh Tran, Stephan Mandt, Jasper Snoek, Tim Salimans, Rodolphe Jenatton, and Sebastian Nowozin. How good is the Bayes posterior in deep neural networks really? In *Proceedings of the 37th International Conference on Machine Learning*, volume 119 of *Proceedings of Machine Learning Research*, pages 10248–10259. PMLR, 13–18 Jul 2020.

- [88] Luong-Ha Nguyen and James-A. Goulet. cuTAGI: a CUDA library for Bayesian neural networks with tractable approximate Gaussian inference. <https://github.com/lhnguyen102/cuTAGI>, 2022.
- [89] Luong-Ha Nguyen and James-A. Goulet. Analytically tractable hidden-states inference in bayesian neural networks. *Journal of Machine Learning Research*, 23(50):1–33, 2022.
- [90] Bai Cong, Nico Daheim, Yuesong Shen, Daniel Cremers, Rio Yokota, Mohammad Emtiyaz Khan, and Thomas Möllenhoff. Variational low-rank adaptation using ivon, 2024.
- [91] Yuesong Shen, Nico Daheim, Bai Cong, Peter Nickl, Gian Maria Marconi, Bazan Clement Emile Marcel Raoul, Rio Yokota, Iryna Gurevych, Daniel Cremers, Mohammad Emtiyaz Khan, and Thomas Möllenhoff. Variational learning is effective for large deep networks. In Ruslan Salakhutdinov, Zico Kolter, Katherine Heller, Adrian Weller, Nuria Oliver, Jonathan Scarlett, and Felix Berkenkamp, editors, *Proceedings of the 41st International Conference on Machine Learning*, volume 235 of *Proceedings of Machine Learning Research*, pages 44665–44686. PMLR, 21–27 Jul 2024.
- [92] J. Heiss, J. Teichmann, and H. Wutte. How infinitely wide neural networks can benefit from multi-task learning - an exact macroscopic characterization. *arXiv preprint arXiv:2112.15577*, 2022.
- [93] J. Heiss. *Inductive Bias of Neural Networks and Selected Applications*. Doctoral thesis, ETH Zurich, Zurich, 2024.
- [94] S. Müller, N. Hollmann, S. P. Arango, J. Grabocka, and F. Hutter. Transformers can do bayesian inference. *arXiv preprint arXiv:2112.10510*, 2021.
- [95] N. Hollmann, S. Müller, L. Purucker, A. Krishnakumar, M. Körfer, S. B. Hoo, R. T. Schirrmeister, and F. Hutter. Accurate predictions on small data with a tabular foundation model. *Nature*, 01 2025.
- [96] S. B. Hoo, S. Müller, D. Salinas, and F. Hutter. The tabular foundation model tabPFN outperforms specialized time series forecasting models based on simple features, 2025.
- [97] L. Guan. Localized conformal prediction: a generalized inference framework for conformal prediction. *Biometrika*, 110:33–50, 2022.
- [98] R. Dwivedi, Y. Tan, B. Park, M. Wei, K. Horgan, D. Madigan, and B. Yu. Stable discovery of interpretable subgroups via calibration in causal studies (stadisc). *International Statistical Review*, 2020.
- [99] L. Buitinck, G. Louppe, M. Blondel, F. Pedregosa, A. Mueller, O. Grisel, V. Niculae, P. Prettenhofer, A. Gramfort, J. Grobler, R. Layton, J. VanderPlas, A. Joly, B. Holt, and G. Varoquaux. API design for machine learning software: experiences from the scikit-learn project. In *ECML PKDD Workshop: Languages for Data Mining and Machine Learning*, pages 108–122, 2013.
- [100] J. Bodik and V. Chavez-Demoulin. Structural restrictions in local causal discovery: identifying direct causes of a target variable. *Biometrika (to appear)*, 2025.
- [101] Jing Lei, Max G’Sell, Alessandro Rinaldo, Ryan J Tibshirani, and Larry Wasserman. Distribution-free predictive inference for regression. *Journal of the American Statistical Association*, 113(523):1094–1111, 2018.
- [102] Matteo Gasparin and Aaditya Ramdas. Merging uncertainty sets via majority vote, 2024.
- [103] D. De Cock. Ames, iowa: Alternative to the boston housing data as an end of semester regression project. *Journal of Statistics Education*, 19(3), 2011.
- [104] Erwan Scornet, Gérard Biau, and Jean-Philippe Vert. Consistency of random forests. *The Annals of Statistics*, 43(4):1716 – 1741, 2015.
- [105] Tong Zhang and Bin Yu. Boosting with early stopping: Convergence and consistency. *The Annals of Statistics*, 33(4):1538 – 1579, 2005.

- [106] Ingo Steinwart and Andreas Christmann. Estimating conditional quantiles with the help of the pinball loss. *Bernoulli*, 17(1):211 – 225, 2011.
- [107] G. De Ath, R. M. Everson, A. A. M. Rahat, and J. E. Fieldsend. Greed is good: Exploration and exploitation trade-offs in bayesian optimisation. *ACM Trans. Evol. Learn. Optim.*, 1(1), April 2021.
- [108] J. Weissteiner, J. Heiss, J. Siems, and S. Seuken. Bayesian optimization-based combinatorial assignment. *Proceedings of the AAAI Conference on Artificial Intelligence*, 37, 2023.

Table 2: List of notable abbreviations used in main the paper.

Abbreviation	Full Term	Description / Citation
PCS	Predictability, Computability, and Stability	Framework for veridical data science [31, 24].
CQR	Conformalized Quantile Regression	Distribution-free prediction intervals [4, 7].
ALEATORIC	Bootstrapped CQR	CQR variant, where we compute CQR on bootstrapped data and taking the median as final estimate. Follows from PCS framework [24]
ALEATORIC-R	Residual-based Bootstrapped CQR	ALEATORIC applied on residuals $Y_i - \hat{f}(X_i)$, where \hat{f} is obtained from PCS.
UACQR	Uncertainty aware CQR	Method from [19] with two variants UACQR-S and UACQR-P
QRF	Quantile Random Forests	Tree-based model for quantile estimation [34].
QXGB	Quantile XGBoost	Gradient boosting for quantile estimation.
GAM	Generalized Additive Model	Used for expectile or quantile regression [60].
PICP	Prediction Interval Coverage Probability	Fraction of targets within predicted intervals.
NIW	Normalized Interval Width	Average interval width normalized by target range.
NCIW	Normalized Calibrated Interval Width	NIW after test-time calibration.
RMSE	Root Mean Squared Error	Average of squared prediction errors.
MAE	Mean Absolute Error	Average of absolute prediction errors.
$\mathcal{N}(0, 1)$	Standard Normal Distribution	Gaussian distribution with mean 0 and variance 1.
supp	support	Support of a distribution or function.

List of Appendices

A	Related Literature	18
A.1	Literature that implicitly assumes $\gamma_1 = 1$ when combining epistemic and aleatoric uncertainty	18
A.2	Literature that implicitly assumes $\lambda = 1$ when combining epistemic and aleatoric uncertainty	18
A.3	Bayesian Models	20
A.4	Bayesian Neural Networks (BNNs)	20
A.5	Conformal Literature that does not account for Epistemic and Aleatoric Uncertainty	21
B	CLEAR Algorithm Details	21
C	Experimental Setup: Details	21
C.1	Additional Baselines	21
C.2	PCS Implementation Details	22
C.3	Metrics	23
D	Simulations	24
D.1	Heteroskedastic Case	24
D.2	Multivariate case	24
E	Full results on real-world datasets	26
E.1	Variant (a)	28
E.2	Variant (b)	30
E.3	Variant (c)	33
E.4	Comparing all variants of CLEAR	36
F	Case Study: Housing Market Price Prediction and changing the number of predictors	37
G	Theory: coverage guarantees for CLEAR	38
G.1	Finite-sample marginal coverage for CLEAR	38
G.2	Asymptotic conditional coverage for CLEAR — discussion of the assumptions in Lemma 2.1	39
H	On the Role of Relative and Absolute Uncertainty in Coverage Guarantees	40
H.1	Metrics and their focus	40
H.2	Applications	40
H.3	Methods	41
H.4	Calibration Techniques	41
H.5	Achieving Conditional Coverage	41

A Related Literature

In the main paper, Section 1 provides a high-level overview of uncertainty quantification in ML. Section 2.2 contains a quick overview of epistemic uncertainty, and Section 2.3 discusses the aleatoric uncertainty. In this appendix, we discuss these concepts in more depth. For an introduction to epistemic and aleatoric uncertainty, see [11], which provides a comprehensive overview.

A.1 Literature that implicitly assumes $\gamma_1 = 1$ when combining epistemic and aleatoric uncertainty

UACQR, introduced by [19], is conceptually closest to CLEAR. Conceptually on a high level, this method corresponds to a variant of CLEAR where $\gamma_1 = 1$ is fixed, and only λ is tuned. This is justified when aleatoric uncertainty is well-calibrated, which may often hold asymptotically. When validation dataset is very small, setting $\gamma_1 = 1$ can even bring small advantages compared to tuning γ_1 . In practice, however, aleatoric uncertainty is often miscalibrated due to over- or under-regularization. Tuning γ_1 helps correct its scale. Furthermore, it can happen in practice that the estimator of the aleatoric uncertainty has a much lower or much higher quality than the epistemic uncertainty. In this case, optimizing both parameters γ_1 and λ allows us to compensate for the failure of one of the two uncertainties to some extent by putting more weight on the other type of uncertainty without changing the marginal coverage. This results in a higher robustness and stability of CLEAR.

Empirical Comparison When comparing against UACQR, we see in Tables 18 to 20 that the performance of CLEAR is much more reliable across the considered datasets and metrics. E.g., on the airfoil, energy efficiency and naval propulsion CLEAR is approximately 2 to 3 times better in metrics such as Quantile Loss, NCIW and Average Interval Score Los, while UACQR never outperforms CLEAR by more than 27% in any of the datasets in any of the considered metrics. Sometimes UACQR-P can also output infinitely wide predictive intervals [19, p. 5], which we observed for one dataset in our experiments. CLEAR performs better than both versions of UACQR in 14 out of 17 datasets. These large difference in performance in Appendix E.3 can partially be explained by our approach to fit the aleatoric uncertainty on the residuals. However, in Appendices E.1 and E.2 every method uses exactly the same module for estimating the point prediction \hat{f} , the uncalibrated epistemic uncertain q^{epi} and the uncalibrated q^{ale} . This allows us to only compare the high-level concepts of fixing $\gamma_1 = 1$ versus optimizing both γ_1 and λ . In this case the gap narrows down substantially, but still CLEAR is more robust. Fixing $\gamma_1 = 1$ can never outperform CLEAR by more than 10% on any dataset with respect to any metric. We hypothesize that CLEAR is more stable and robust since it can compensate for shortcomings of the base models more easily: If the aleatoric uncertainty is overestimated or underestimated, CLEAR can correct its scale by adjusting γ_1 .

A.2 Literature that implicitly assumes $\lambda = 1$ when combining epistemic and aleatoric uncertainty

Most of the literature that combines epistemic and aleatoric uncertainty implicitly assumes that $\lambda = 1$, when they simply combine epistemic and aleatoric uncertainty in the ration 1:1. On top of the resulting uncertainty once can use (conformal) calibration, which corresponds to CLEAR’s calibration of γ_1 . However, in contrast to CLEAR, they do not rebalance the ratio of epistemic and aleatoric uncertainty with λ .

In practice, it is possible to underestimate the aleatoric uncertainty and overestimate epistemic uncertainty. This results in a one-dimensional calibration via γ_1 , and consequently, narrow intervals in regions of dominating aleatoric uncertainty or in wide intervals in regions of dominating epistemic uncertainty. γ_1 alone cannot solve this alone. CLEAR can deal well with such situations by compensating for such an imbalance via λ .

A.2.1 Deep Ensembles

While it is quite common to refer to *deep ensembles* (DE), whenever one uses an ensemble of neural networks (NNs) for uncertainty estimation, it is important to note that [22] introduced DE as a method which both estimates epistemic and aleatoric uncertainty. For regression, they train each NN with

2 outputs estimating μ and σ via a Gaussian Maximum-Likelihood-loss (as in [35]), where σ is responsible for the aleatoric uncertainty, which they refer to as “ambiguity in targets y for a given x ”. Moreover, they use the ensemble diversity to estimate epistemic uncertainty, which they refer to as “model uncertainty”. Although DE is mainly known for its ensembling approach, [22, Table 2 in Appendix A.1] clearly shows that both the aleatoric and epistemic parts are crucial in terms of empirical performance. In their paper, the authors do not apply any calibration on top, i.e., as it is implicitly assumed that $\gamma_2 = \gamma_1 = 1 = \lambda$. However, it is common to apply (conformal) calibration on top. The commonly used calibration techniques only calibrate γ_1 , while keeping $\lambda = 1$ fixed, in contrast to CLEAR. In particular, for DE, both the diversity of the ensemble and the bias on aleatoric are very sensitive to various hyperparameters. One type of uncertainty may be strongly under-estimated. In contrast, the other type is strongly over-estimated, which motivates the need to calibrate explicitly calibrate λ in a data-driven way.

Technical Details on Adversarial Attacks for Deep Ensembles. The original paper [22] is written as if applying adversarial attacks is an integral part of DEs and one of the paper’s main contributions. However, to the best of our knowledge, many practitioners refer to “DEs” without implying adversarial attacks during training, and adversarial attacks during training are seen as an optional add-on to DEs but not an important part of DEs. Furthermore, the regression results in [22, Table 2 in Appendix A.1] do not suggest that adversarial attacks during training are particularly beneficial to the performance.

Technical Details on Measuring Deep Ensemble’s diversity. Intuitively, one should estimate high epistemic uncertainty if there is a significant disagreement among the ensemble’s predictions and small epistemic uncertainty if they agree. While [24, Chapter 13] and [23] suggest using quantiles, [22] suggest using the empirical standard deviation to estimate DE’s disagreement among ensemble’s predictions. It seems plausible that in [22]’s case of 5 ensemble members, using the standard deviation and some Gaussian assumptions can be more appropriate while in [24, Chapter 13]’s and [23]’s case of 100 or more ensemble members, quantiles can be more accurate.

Variations of Deep Ensembles. There exist several modifications of DE that, for example, promote the ensemble’s diversity on the function space via an additional loss term during training [76], ensemble over multiple different hyperparameters [77], or reduce the computational training cost [17, 27, 78, 79, 19, 23].

A.2.2 Monte Carlo Dropout

[27] originally studied Monte Carlo Dropout (MC Dropout) without explicitly modeling aleatoric uncertainty, which was then extended by [17] to also explicitly model aleatoric paper. While [27] see MC Dropout as an approximation of a Bayesian neural network, one can also see it as another ensemble method. The main difference to DE is that MC Dropout only trains one NN with dropout and obtains an ensemble after training by randomly setting weights of the model to zero at inference time. Analogously to DE, MC Dropout also adds epistemic and aleatoric uncertainty in the ratio 1:1 with the same disadvantages as described before in Appendix A.2.1.

A.2.3 “A Deeper Look into Aleatoric and Epistemic Uncertainty Disentanglement”

[80] empirically concludes that ensembles have the best uncertainty and disentangling behavior of epistemic and aleatoric uncertainty. In their paper, the authors do not use any form of calibration. This would correspond to $\gamma_2 = \gamma_1 = 1 = \lambda$ in our notation. Their paper suggests a different loss function, which they call β -NLL, for training to mitigate the underestimation of aleatoric uncertainty to some extent in their experimental setting without comparing this approach to calibration. In [80, Figure 6], one can observe that even without the β -NLL, both epistemic and aleatoric uncertainty already have a good shape (that is, good relative uncertainty, see Appendix H) for deep ensembles (DE). The main problem of DE in [80, Figure 6] is that the epistemic uncertainty is too small by a very large factor (that is, poor absolute scale of uncertainty, see Appendix H), while aleatoric uncertainty has already almost the correct scaling. From our perspective, applying CLEAR on their DE would probably largely fix their problem of DE if CLEAR chooses $\gamma_1 \approx 1$ and $\lambda \gg 1$. However, they show that for this specific experiment, β -NLL also fixes the problem. In general, where one suspects that the aleatoric or the epistemic uncertainty might be too small or too large across the domain, we strongly recommend simply applying CLEAR on top of the already trained ensemble instead of retraining

all the models with a new training pipeline. The concept of CLEAR can be implemented in a few minutes and calibrates an already trained ensemble in a few seconds. We considered an interesting open problem to study if β -NLL can improve the relative epistemic and aleatoric uncertainty (see Appendix H).

A.2.4 “Recalibration of Aleatoric and Epistemic Regression Uncertainty in Medical Imaging”

[14] also combines epistemic and aleatoric uncertainty in the ratio 1:1 and applies a single constant (corresponding to γ_1 in our notation) to scale the total predictive uncertainty, which corresponds to fixing $\lambda = 1$ resulting in the same potential for problems as mentioned before.

A.3 Bayesian Models

If one had access to a perfect prior, perfectly computed Bayesian inference, it would provide well-calibrated epistemic and aleatoric uncertainty, at least in theory. However, in practice, the ratio of estimated epistemic and aleatoric uncertainty can be very wrong, and the uncertainty can be miscalibrated.

A.3.1 Gaussian Process Regression (GPR)

Gaussian Process regression [81] provides a closed form for exact posterior epistemic uncertainty for a given Gaussian process as a prior and for a given known noise Gaussian noise distribution. If the (scale of the) prior or the scale (of the noise) is misspecified, the ratio of estimated epistemic and aleatoric uncertainty can be arbitrarily bad, and the uncertainty can be miscalibrated. Therefore, it is common to optimize hyperparameters like the noise scale and the prior scale (typically in a non-Bayesian way). The main differences to CLEAR are that 1) for GPR, one has to refit the model for every considered possibility of hyperparameters, while CLEAR optimizes γ_1 and λ after fitting the model, resulting in much lower computational costs; 2) CLEAR can be applied to other base models as well such as tree-based models which are more popular in many applications; 3) standard implementations of GPR fit the hyperparameter on the training data rather than on the validation data.

A.4 Bayesian Neural Networks (BNNs)

Bayesian neural networks [29, 82] offer a principled Bayesian framework for quantifying both epistemic and aleatoric uncertainty through the placement of a prior distribution on network weights. As for GPR, the ratio of estimated epistemic and aleatoric uncertainty in BNNs is highly sensitive to the choice of prior. Consequently, we advocate applying CLEAR to an already trained BNN, calibrating both uncertainty types via scaling factors γ_1 and γ_2 with negligible additional computational overhead. While exact Bayesian inference in large BNNs is computationally intractable, numerous approximation techniques have been proposed [83–85, 27, 22, 30, 86, 28, 87–91]. Interestingly, theoretical [92, 93] and empirical [87] studies suggest that some of these approximations can actually provide superior estimates compared to their exact counterparts, due to poor choices of priors, such as i.i.d. Gaussian priors, in certain settings.

A.4.1 EPISCORE

The recent work by [20] introduces EPISCORE. Similar to our work, this method addresses the limitations of standard conformal prediction in capturing epistemic uncertainty. EPISCORE focuses on enhancing existing conformal scores with Bayesian epistemic uncertainty. They also compute the average interval score for 95% predictive intervals on the datasets *airfoil* (where their best method out of 6 variants performs more than 2 times worse than the worst of the 3 variants of CLEAR), *concrete* (where their best method performs more than 1.5 times worse than the worst variant of CLEAR) and *Superconductivity* (where their best method performs approximately 1.3 times worse than the worst variant of CLEAR).

A.4.2 TabPFN

TabPFN [94, 95] is a transformer trained to emulate Bayesian inference over a diverse prior of realistic tabular problems, achieving strong predictive uncertainty estimates with a single forward

pass. Its prior spans diverse noise structures and function classes, yielding uncertainty estimates that inherently mix aleatoric and epistemic components. Although recent variants such as TabPFN-TS [96] extend its applicability to time series, the method is limited to small tabular datasets and does not disentangle uncertainty types. In contrast, our approach explicitly separates and calibrates epistemic and aleatoric uncertainty and scales to arbitrary modalities and data sizes.

A.5 Conformal Literature that does not account for Epistemic and Aleatoric Uncertainty

The classical conformal prediction literature [4, 6, 25, 9, 8] primarily focuses on achieving marginal coverage, often with attention to asymptotic conditional coverage. However, it often overlooks epistemic uncertainty, which is especially critical in finite-sample settings. While [26] established the impossibility of achieving exact distribution-free conditional coverage in finite samples, several recent works attempt to improve coverage guarantees in more restricted settings under certain assumptions. For instance, [10] propose coverage guarantees over a subclass of distribution shifts, effectively interpolating between marginal and conditional coverage. Others, such as [97] and [98], provide guarantees over a finite set of prespecified subgroups. We argue that to obtain reliable conditional coverage, one must model the uncertainty arising from each stage of the data science life cycle [24], and appropriately integrate these uncertainties to achieve meaningful coverage guarantees.

B CLEAR Algorithm Details

Algorithm 2 Fast Conformal Implementation of Step 3 from Algorithm 1

1: **Input:** Data (X_i, Y_i) for $i = 1, \dots, n$, split into training $\mathcal{D}_{\text{train}}$, calibration \mathcal{D}_{cal} , and validation \mathcal{D}_{val} (we consider $\mathcal{D}_{\text{cal}} = \mathcal{D}_{\text{val}}$); grid of λ values Λ ; significance level α .

2: **Step 3: Define prediction intervals for each $\lambda \in \Lambda$.**

First, define a preliminary (non-calibrated) interval:

$$\tilde{C}_\lambda = \left[\hat{f} - \hat{q}_{\alpha/2}^{\text{ale}} - \lambda \hat{q}_{\alpha/2}^{\text{epi}}, \hat{f} + \hat{q}_{1-\alpha/2}^{\text{ale}} + \lambda \hat{q}_{1-\alpha/2}^{\text{epi}} \right]$$

Then, compute conformity scores $S_i^\lambda = \max \left\{ \frac{\tilde{l}_\lambda(X_i) - Y_i}{\hat{f}(X_i) - \tilde{l}_\lambda(X_i)}, \frac{Y_i - \tilde{u}_\lambda(X_i)}{\tilde{u}_\lambda(X_i) - \hat{f}(X_i)} \right\}$, where $\tilde{l}_\lambda(x), \tilde{u}_\lambda(x)$ are the lower and upper bounds of $\tilde{C}_\lambda(x)$. Let γ_1 be the $\lceil (1 - \alpha)(|\mathcal{D}_{\text{cal}}| + 1) \rceil$ -th smallest score among $\{S_i^\lambda\}$ (if $\lceil (1 - \alpha)(|\mathcal{D}_{\text{cal}}| + 1) \rceil > |\mathcal{D}_{\text{cal}}|$, take the largest score). Define the calibrated interval:

$$C_\lambda = \left[\hat{f} - \gamma_1 \hat{q}_{\alpha/2}^{\text{ale}} - \lambda \gamma_1 \hat{q}_{\alpha/2}^{\text{epi}}, \hat{f} + \gamma_1 \hat{q}_{1-\alpha/2}^{\text{ale}} + \lambda \gamma_1 \hat{q}_{1-\alpha/2}^{\text{epi}} \right]$$

3: **Output:** calibrated prediction intervals C_λ for each λ from the grid Λ .

C Experimental Setup: Details

C.1 Additional Baselines

The following baselines provide further context and comparisons, omitted from the main paper for brevity. All compared methods (except UACQR) use the same median $\hat{f}(x) = \hat{f}_{\text{PCS}}(x)$ obtained from PCS. (Obviously, all the results from Appendix E.1 use PCS variant (a), from Appendix E.2 use PCS variant (b), from Appendix E.3 use PCS variant (c).) This allows us to isolate the effect of different uncertainty quantification methods.

1. **Conformalized PCS median (Naive):** For the PCS ensemble, we compute the median prediction $\hat{f}(x) = \hat{f}_{\text{PCS}}(x)$ for each x . On the calibration set, absolute residuals $a_i = |y_i - \hat{f}(x_i)|$ are computed. The $(1 - \alpha)$ -th quantile γ_{naive} of these absolute residuals is then used to define the interval:

$$C_{\text{Naive}}(x) = [\hat{f}(x) - \gamma_{\text{naive}}, \hat{f}(x) + \gamma_{\text{naive}}]$$

This method applies a constant, symmetric width adjustment to the point predictions. The result of this baseline has been presented for the simulations. We omit it from the real-world data for brevity. However, all the baselines can be found in the supplementary code.

2. **CLEAR with fixed $\lambda = 1$:** This is a variant of the main CLEAR methodology where the ratio $\lambda = \gamma_2/\gamma_1$ is fixed to 1. This implies $\gamma_1 = \gamma_2$. The prediction interval, based on Equation (3), becomes:

$$C_{\lambda=1}(x) = \left[\hat{f}(x) - \gamma_1 \left(\hat{q}_{\alpha/2}^{\text{ale}}(x) + \hat{q}_{\alpha/2}^{\text{epi}}(x) \right), \quad \hat{f}(x) + \gamma_1 \left(\hat{q}_{1-\alpha/2}^{\text{ale}}(x) + \hat{q}_{1-\alpha/2}^{\text{epi}}(x) \right) \right].$$

In this configuration, the single parameter γ_1 is calibrated using the standard split conformal procedure on the validation set. It effectively learns a single scaling factor for the sum of the pre-calibrated aleatoric and epistemic uncertainty widths, without adjusting their ratio.

3. **CLEAR with fixed $\gamma_1 = 1$:** Another variant of CLEAR where γ_1 is fixed to 1. With $\gamma_1 = 1$, then $\gamma_2 = \lambda$ and the prediction interval from Equation (3) reads as:

$$C_{\gamma_1=1}(x) = \left[\hat{f}(x) - \hat{q}_{\alpha/2}^{\text{ale}}(x) - \lambda \hat{q}_{\alpha/2}^{\text{epi}}(x), \quad \hat{f}(x) + \hat{q}_{1-\alpha/2}^{\text{ale}}(x) + \lambda \hat{q}_{1-\alpha/2}^{\text{epi}}(x) \right].$$

Here, λ (or equivalently γ_2) is the parameter calibrated on the calibration set through a coverage-based adjustment. This approach fixes the contribution of the (pre-calibrated) aleatoric uncertainty component and adaptively scales the epistemic uncertainty component.

4. **UACQR-S and UACQR-P** For variant (c), instead of computing $C_{\gamma_1=1}(x)$ and $C_{\lambda=1}(x)$ with CLEAR, we directly use the implementation from [19] to assess our performance against this alternative. Since this is only relevant for variant (c), we use the exact same configuration as the aleatoric part for QRF (see the following subsection and Table 3).

C.2 PCS Implementation Details

This section outlines the specific implementation details for generating the PCS ensembles, which provide the point predictor \hat{f} and the raw epistemic uncertainty estimates \hat{q}^{epi} used as input for the CLEAR method (Section 2.4), and also form the basis for the standalone calibrated PCS baseline intervals. We explicitly opted for experimenting with three variants of CLEAR to assess the framework’s performance and robustness across different modeling choices for epistemic and aleatoric uncertainty components, as discussed in the main text. The core methodology, involving model selection and model perturbations via bootstrapping to capture epistemic uncertainty, follows the principles described in Section 2.

The process begins with data partitioning and bootstrapping. For each dataset and unique random seed, the data is divided into training (60%), validation (20%), and test (20%) sets. Subsequently, $n_{\text{boot}} = 100$ bootstrap resamples are drawn from this designated training set to construct the PCS ensemble. Then, for our variants, two distinct pools of base models were developed to generate these PCS ensembles, catering to the different CLEAR variants. Table 3 details the quantile estimators used for CLEAR variant (a). Variant (b) only uses QXGB from Table 3. Table 4 describes the mean estimators utilized for CLEAR variant (c).

Table 3: Base models and key hyperparameters for the quantile models used in CLEAR variants (a). Variant (b) uses only QXGB from this table. All models target the conditional median ($\tau = 0.5$).

Model	Key Hyperparameters	Ref.
QRF	100 trees, min. leaf size: 10	[34]
QXGB	100 trees, tree method: histogram, min. child weight: 10	[59]
Expectile GAM	10 P-splines (order 3), smoothing parameter optimized via CV (5 min. timeout)*	[60]

*Included only if hyperparameter optimization converged successfully, otherwise using the default values.

Ensemble Construction and Model Selection: For each of the $n_{\text{boot}} = 100$ bootstrap samples, all models within the relevant pool (median estimators for variants a/b, mean estimators for variant

Table 4: Base models and key hyperparameters for the mean estimators (used in CLEAR variant c). All models target the conditional mean and are from Scikit-learn [99], except XGBoost, which is from [59]. All unspecified hyperparameters use the Scikit-learn defaults.

Category	Model	Key Hyperparameters
Linear Models	Ordinary Least Squares	Default
	Ridge	Default alphas (CV)
	Lasso	3-fold CV
	ElasticNet	3-fold CV
Tree Ensembles	Random Forest	100 trees, min. leaf size: 5, max. features: 0.33
	Extra Trees	Same hyperparameters as random forest
	AdaBoost	Default
	XGBoost	Default
Neural Network	MLP	Single hidden layer (64 neurons)

c) were trained. The single best-performing model type ($k = 1$) was then identified based on the lowest RMSE achieved on the held-out validation set. Consequently, the final PCS ensemble for each random seed comprised 100 instances of this selected top-performing model type. Specifically, CLEAR variant (a) considered all models from Table 3 for this selection process, variant (b) was restricted to selecting always QXGB from this pool, and variant (c) considered all the models from Table 3 instead. All models used default parameters from their respective libraries unless otherwise specified in the tables, and random states were fixed to ensure reproducibility.

Derivation of \hat{f} and \hat{q}^{epi} for CLEAR: The point predictor $\hat{f}(x)$ and the raw epistemic uncertainty contributions $\hat{q}_{\alpha/2}^{\text{epi}}(x)$ and $\hat{q}_{1-\alpha/2}^{\text{epi}}(x)$ supplied to the CLEAR method are derived from this final ensemble of 100 model instances. As detailed in Section 2.2, $\hat{f}(x)$ is the pointwise empirical median of the ensemble’s predictions. The epistemic uncertainty terms represent the pointwise distances from this median to the ensemble’s empirical $\alpha/2$ and $1 - \alpha/2$ quantiles, respectively.

Calibration of the Standalone PCS Baseline: The standalone PCS baseline method involves a distinct calibration process. From the ensemble’s raw pointwise $\alpha/2$ and $1 - \alpha/2$ quantile predictions ($\hat{f}_{\alpha/2}(x)$ and $\hat{f}_{1-\alpha/2}(x)$), a single, global multiplicative calibration factor, γ_{PCS} , is computed. This γ_{PCS} is the smallest value ensuring that prediction intervals, formed by scaling the raw epistemic uncertainty around $\hat{f}(x)$ (i.e., $[\hat{f}(x) - \gamma_{\text{PCS}}(\hat{f}(x) - \hat{f}_{\alpha/2}(x)), \hat{f}(x) + \gamma_{\text{PCS}}(\hat{f}_{1-\alpha/2}(x) - \hat{f}(x))]$), achieve the target $1 - \alpha$ coverage on the validation set, incorporating the standard finite-sample correction. This γ_{PCS} is then applied to generate the PCS baseline intervals on the test set. It is important to reiterate that this γ_{PCS} is separate and computed independently from γ_1 and λ parameters optimized within the CLEAR framework.

C.3 Metrics

This appendix provides detailed definitions for the evaluation metrics used in the main paper. We consider test data $(X_i, Y_i)_{i=1}^N$ and prediction intervals $[L_i, U_i]$.

- **Prediction Interval Coverage Probability (PICP):** Measures the proportion of true values falling within the predicted intervals, calculated as:

$$\text{PICP}(L, U) = \frac{1}{N} \sum_{i=1}^N \mathbb{1}_{[L_i, U_i]}(Y_i)$$

where $\mathbb{1}_{[L_i, U_i]}(Y_i)$ is the indicator function; it equals 1 if $Y_i \in [L_i, U_i]$ and 0 otherwise.

- **Normalized Interval Width (NIW):** Quantifies the average width of prediction intervals normalized by the range of the target variable:

$$\text{NIW}(L, U) = \frac{\frac{1}{N} \sum_{i=1}^N (U_i - L_i)}{\max(Y) - \min(Y)}$$

- **Quantile Loss (also known as pinball loss):** Evaluates the accuracy of predicted quantiles by penalizing both under- and overestimation. It reflects a trade-off between coverage (PICP) and interval width (NIW), rewarding narrow intervals that still maintain proper coverage. For a given quantile level τ , the quantile loss function is:

$$QL_\tau(y, q) = (y - q)(\tau - \mathbb{1}_{(-\infty, q]}(y)),$$

where q is the predicted τ -quantile. For prediction intervals at level $1 - \alpha$, we evaluate this at both $\tau = \alpha/2$ and $\tau = 1 - \alpha/2$ using

$$QuantileLoss(L, U) = \sum_{i=1}^N [QL_{\alpha/2}(Y_i, L(X_i)) + QL_{1-\alpha/2}(Y_i, U(X_i))] / 2.$$

- **Average Interval Score Loss (AISL)** [61]: This score balances interval width with coverage penalties, defined as

$$AISL(L, U) = \frac{1}{N} \sum_{i=1}^N \left[(U_i - L_i) + \frac{2}{\alpha} (L_i - Y_i) \mathbb{1}\{Y_i < L_i\} + \frac{2}{\alpha} (Y_i - U_i) \mathbb{1}\{Y_i > U_i\} \right],$$

where $\mathbb{1}\{\cdot\}$ is the indicator function.

D Simulations

For each simulation run, the coefficients β_1, \dots, β_d are drawn independently from a Gaussian distribution $\mathcal{N}(1, 0.5^2)$. The mean function $\mu(X)$ is then defined as $\mu(X) = 5.0 + \sum_{i=1}^d (-1)^{i+1} \beta_i |X_i|^{e_i}$, where the exponent $e_i = 1.5$ if i is odd, and $e_i = 1.25$ if i is even.

D.1 Heteroskedastic Case

In Section 3.1, we focused on the univariate homoskedastic setting ($d = 1$ and $\sigma(x) = 1$). Here, we briefly report results for heteroskedastic data, which show similar patterns. Figures 4 and 5 illustrate the conditional coverage and interval width of the algorithms under two heteroskedastic noise structures: $\sigma_2(x) = 1 + |x|$ and $\sigma_3(x) = 1 + \frac{1}{1+x^2}$. As mentioned, the results are analogous to the homoskedastic setting in Section 3.1.

D.2 Multivariate case

D.2.1 Test point generation

Following setup in [100], let $r_1 < r_2 < \dots < r_K$ denote a set of predetermined distances. For each radius r_k , we sample points uniformly from the surface of the unit d -dimensional sphere as follows. First, we draw a vector $\mathbf{v} \in \mathbb{R}^d$ whose entries are independent standard normal random variables. We then normalize \mathbf{v} to obtain a unit vector $\mathbf{u} = \mathbf{v} / \|\mathbf{v}\|_2$. Finally, we scale \mathbf{u} by r_k to obtain the test point $\mathbf{x} = r_k \cdot \mathbf{u}$. In the one-dimensional case, this procedure reduces to selecting $x = r_k$ or $x = -r_k$ with equal probability. This mechanism ensures that, for each r_k , the generated points are uniformly distributed on the surface of the sphere of radius r_k , thereby allowing a precise evaluation of prediction intervals as a function of distance from the origin. Finally, we generate Y with the same data-generating mechanism as in the train set.

D.2.2 Results

Figure 6 illustrates the conditional coverage and interval width of the evaluated algorithms in the multivariate setting, where X is drawn from an independent multivariate Gaussian distribution and $Y = \mu(X) + \varepsilon$, with $\varepsilon \sim \mathcal{N}(0, 1)$. The regression function $\mu(X)$, as previously defined, involves a sum of randomly weighted power transformations of the absolute values of the input features.

Consistent with the univariate homoskedastic results in Section 3.1, Figure 6 shows that both CQR and naive conformal prediction achieve reliable coverage in high-density regions but tend to under-cover in low-density or extrapolation areas. In contrast, CLEAR maintains valid conditional coverage across the entire input space by appropriately adjusting interval widths.

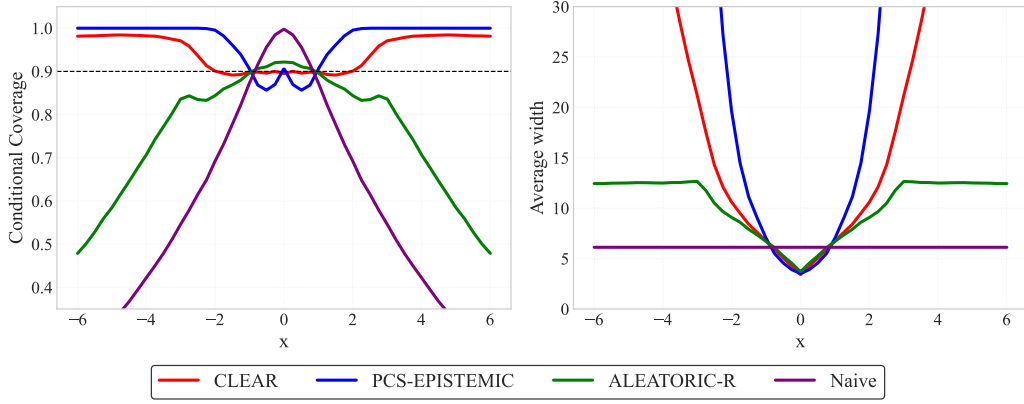


Figure 4: Univariate conditional coverage and average width of the prediction intervals for a heteroskedastic case where $\sigma_2(x) = 1 + |x|$.

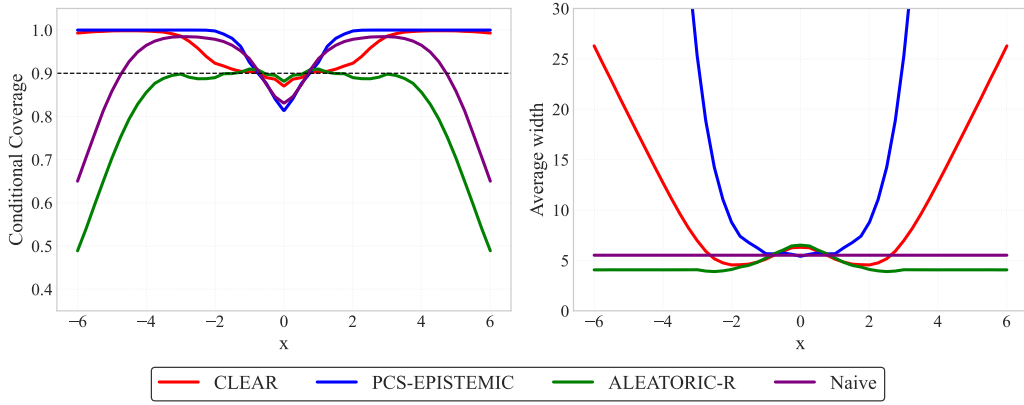


Figure 5: Univariate conditional coverage and average width of the prediction intervals for a heteroskedastic case where $\sigma_3(x) = 1 + \frac{1}{1+x^2}$.

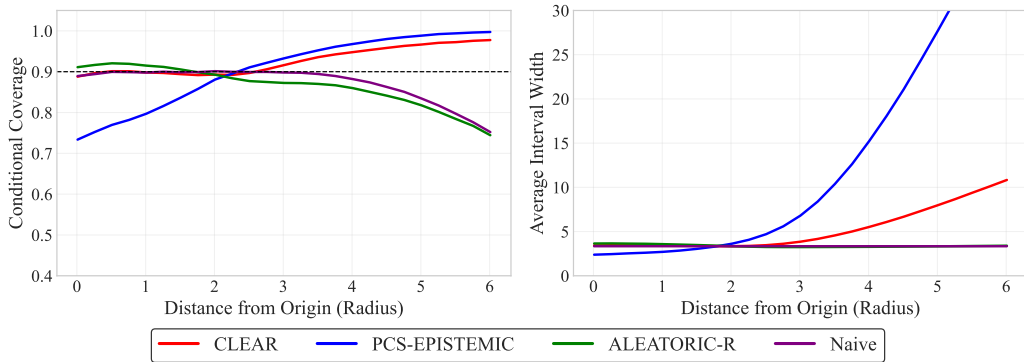


Figure 6: Multivariate conditional coverage and average width (distance from the origin is shown) of the prediction intervals for a homoskedastic case where $d \in \{1, 2, 3, 20\}$ was randomly selected.

E Full results on real-world datasets

This appendix presents the detailed quantitative results from the benchmark experiments conducted on the 17 real-world datasets, complementing the summary findings in the main paper (Section 4.2). Description of the datasets can be found in Table 5. As a reminder, we evaluate three distinct configurations (variants) of our proposed CLEAR method alongside the baseline approaches (PCS, ALEATORIC, ALEATORIC-R). The differences among these 3 variants are considered base models. For each variant, CLEAR is applied on the already trained PCS and uncalibrated ALEATORIC-R. To recap these variants:

- **Variant (a):** Employs a quantile PCS approach using a diverse pool of quantile estimators (QRF, QXGB, Expectile GAM¹) for estimating the conditional medians based on the bootstraps. The top-performing model type ($k = 1$) on the validation set is selected. 1) Based on the selected model type, we compute the epistemic component \hat{q}^{epi} (via empirical quantiles over the estimated medians from the $b = m$ bootstraps) and the median \hat{f} (as empirical median over the estimated medians). 2) Using the same selected quantile model type, the aleatoric component \hat{q}^{ale} is derived from a bootstrapped ALEATORIC-R model.
- **Variant (b):** Similar to (a), but restricts the model pool for both PCS and the paired ALEATORIC-R exclusively to QXGB.
- **Variant (c):** Uses a standard PCS approach with mean-based regression models (e.g., Random Forest, XGBoost) for the epistemic component (via empirical quantiles over the estimated medians) and median prediction \hat{f} (as empirical median over the estimated means), selecting the top model ($k = 1$). The aleatoric component is derived from a bootstrapped ALEATORIC-R model using QRF.

The subsequent subsections present the comprehensive results for each variant (a, b, c). All experiments were run across 10 different random seeds², and the results on the test set are presented. The subsequent tables report the average performance metric across these 10 seeds, along with the standard deviation ($\pm\sigma$), to indicate the variability associated with data splitting. For each variant, we provide tables detailing the metrics presented in Appendix C.3 for all methods across all datasets at a 95% nominal coverage level. Lower values are preferable for all metrics except PICP, which should ideally be close to the target of 0.95. Additionally, summary plots (Figures 3, 7 and 8) visualize the relative NCIW and Quantile Loss performance normalized against the respective CLEAR variant baseline. Additionally, only for variant (c), we provide Table 21 with the values of λ and γ_1 to provide some insights into the aleatoric/epistemic allocations of CLEAR. Finally, Figure 9 (Appendix E.4) provides a direct comparison of the NCIW and Quantile Loss between the three CLEAR variants themselves, using variant (a) as the reference baseline.

Appendix E.4 shows that the primary configuration of CLEAR presented in the main text, variant (a), leverages a diverse set of quantile models for robust epistemic uncertainty estimation and generally delivers the most consistent and superior performance. As detailed in Figure 9 in the appendix, CLEAR in variant (a) tends to marginally outperform the model in variant (b), which is restricted to QXGB, and variant (c), which utilizes standard mean-based PCS models. For instance, in variant (a), QXGB was selected in approximately 64% of cases, QRF in 24%, and ExpectileGAM in the remainder of cases. In variant (c), XGBoost was chosen about 70% of the time, with other models (excluding Ridge) sharing the rest. The importance of this dynamic model selection is evident in datasets like `naval_propulsion`, where variants (b) and (c) can struggle due to their fixed model choices (QXGB and QRF for the aleatoric part, respectively), whereas variant (a) can adapt by selecting, for example, ExpectileGAM. This highlights the stability advantage of CLEAR (a) and the benefit of PCS’s dynamic model choice, especially when the aleatoric component can also adapt. Nevertheless, the CLEAR framework overall demonstrates considerable robustness even with these alternative model choices. For instance, variant (b) still provides NCIW reductions of approximately 17.3% and 4.9% over its corresponding PCS and ALEATORIC-R baselines, respectively (Figure 7). A similar advantage is observed for variant (c) (Figure 8), which reduces NCIW by about 7.6% against ALEATORIC-R, the best-performing variant of CQR that uses our novel residual-based technique.

¹Strictly speaking, Expectile GAM estimates expectiles rather than quantiles. While it is not a consistent estimator for quantiles in theory, mixing expectiles and quantiles may still be practical in applications.

²Due to a bug in pygam’s Expectile GAM [60], for the `naval_propulsion` data in variant (c), one of the runs failed; hence, there are 9 runs available instead of 10.

Detailed motivation behind variant (a). Overall, variant (a) archives the best results (see Figure 9). Therefore, we recommend to use CLEAR variant (a). The experiments in variant (a) are fair, since each of the competing methods uses the same base model, which is selected per data set based on the RMSE on the validation data set. See Appendix E.1 for the results.

Detailed motivation behind variant (b). Variant (b) is the simplest to understand, easiest to implement, and computationally cheapest variant and provides maximal fairness, making it particularly scientifically sound. Each method simply uses QXGB as base model without any model selection step. Strictly speaking, variant (b) is the only variant where ALEATORIC and ALEATORIC-R are fully conformal, since variant (b) uses the calibration data set only for calibration, while variant (a) and (c) reuse the validation set used for model selection as calibration data set. However, in practice, we observe this re-usage does not hurt calibration in any significant way (Table 6 and Table 16). See Appendix E.2 for the results of variant (b).

Detailed motivation behind variant (c). Variant (c) uses the same set of base models as suggested by the authors of PCS uncertainty quantification [23]. [23] conducted extensive experiments showing that PCS uncertainty quantification substantially outperforms popular conformal baselines such as split conformal regression [101], Studentized conformal regression [101], and Majority Vote [102] (by more than 20% on average in terms of interval width). Our experiments showing that CLEAR (a) outperforms CLEAR (c) (Figure 9) and CLEAR (c) outperforms PCS uncertainty quantification (c) (Appendix E.3), together with the experiments by [23], strongly suggests that CLEAR clearly outperforms these popular conformal baselines. See Appendix E.3 for the results of variant (c).

Overall, CLEAR shows the strongest performance across all variants (a), (b) and (c), demonstrating CLEAR’s stability across different settings, data sets, and metrics.

Table 5: Dataset statistics where d represents the number of variables, n represents the number of observations, followed by the minimum, maximum, and range values for y .

Dataset	n	d	y_{min}	y_{max}	y_{range}
aileron	13,750	40	-0.0036	0.00e+00	0.0036
airfoil	1,503	5	104.2040	140.1580	35.9540
allstate	5,000	1037	200.0000	3.31e+04	3.29e+04
ca_housing	20,640	8	1.50e+04	5.00e+05	4.85e+05
computer	8,192	21	0.00e+00	99.0000	99.0000
concrete	1,030	8	2.3300	81.7500	79.4200
elevator	16,599	18	0.0120	0.0780	0.0660
energy_efficiency	768	10	6.0100	43.1000	37.0900
insurance	1,338	8	1121.8739	6.26e+04	6.15e+04
kin8nm	8,192	8	0.0632	1.4585	1.3953
miami_housing	13,932	28	7.20e+04	2.65e+06	2.58e+06
naval_propulsion	11,934	24	0.0690	1.8320	1.7630
parkinsons	5,875	18	7.0000	54.9920	47.9920
powerplant	9,568	4	420.2600	495.7600	75.5000
qsar	5,742	500	-6.2400	11.0000	17.2400
sulfur	10,081	5	0.00e+00	1.0000	1.0000
superconductor	21,263	79	3.25e-04	185.0000	184.9997

E.1 Variant (a)

Table 6: Variant (a) PICP at 95% prediction intervals, aggregated across 10 seeds.

Dataset	CLEAR	ALEATORIC	ALEATORIC-R	PCS-EPISTEMIC	Naive	$\gamma_1 = 1$	$\lambda = 1$
aileron	0.95 \pm 0.00	0.95 \pm 0.00	0.95 \pm 0.00	0.95 \pm 0.01	0.95 \pm 0.01	0.95 \pm 0.00	0.95 \pm 0.00
airfoil	0.95 \pm 0.01	0.95 \pm 0.01	0.95 \pm 0.01	0.95 \pm 0.01	0.95 \pm 0.02	0.95 \pm 0.02	0.95 \pm 0.01
allstate	0.95 \pm 0.01	0.95 \pm 0.01	0.95 \pm 0.01	0.95 \pm 0.01	0.95 \pm 0.01	0.95 \pm 0.01	0.95 \pm 0.01
ca_housing	0.95 \pm 0.01	0.95 \pm 0.01	0.95 \pm 0.01	0.95 \pm 0.01	0.95 \pm 0.01	0.95 \pm 0.01	0.95 \pm 0.01
computer	0.95 \pm 0.01	0.97 \pm 0.01	0.95 \pm 0.01	0.95 \pm 0.01	0.96 \pm 0.01	0.95 \pm 0.01	0.96 \pm 0.01
concrete	0.95 \pm 0.02	0.96 \pm 0.02	0.95 \pm 0.02	0.95 \pm 0.01	0.94 \pm 0.03	0.95 \pm 0.01	0.95 \pm 0.01
elevator	0.95 \pm 0.00	0.95 \pm 0.01	0.95 \pm 0.00	0.95 \pm 0.00	0.95 \pm 0.01	0.95 \pm 0.00	0.95 \pm 0.00
energy_efficiency	0.95 \pm 0.02	0.96 \pm 0.02	0.95 \pm 0.02	0.96 \pm 0.01	0.95 \pm 0.02	0.96 \pm 0.01	0.96 \pm 0.01
insurance	0.95 \pm 0.02	0.96 \pm 0.01	0.96 \pm 0.02	0.95 \pm 0.01	0.95 \pm 0.02	0.96 \pm 0.01	0.96 \pm 0.01
kin8nm	0.95 \pm 0.01	0.95 \pm 0.01	0.95 \pm 0.01	0.95 \pm 0.01	0.95 \pm 0.01	0.95 \pm 0.01	0.95 \pm 0.01
miami_housing	0.95 \pm 0.01	0.95 \pm 0.00	0.95 \pm 0.01	0.95 \pm 0.01	0.95 \pm 0.01	0.95 \pm 0.00	0.95 \pm 0.00
naval_propulsion	0.95 \pm 0.01	0.96 \pm 0.01	0.95 \pm 0.01	0.95 \pm 0.01	0.95 \pm 0.01	0.95 \pm 0.01	0.95 \pm 0.01
parkinsons	0.95 \pm 0.01	0.95 \pm 0.01	0.95 \pm 0.01	0.95 \pm 0.01	0.95 \pm 0.01	0.95 \pm 0.01	0.95 \pm 0.01
powerplant	0.95 \pm 0.01	0.95 \pm 0.00	0.95 \pm 0.01	0.95 \pm 0.01	0.95 \pm 0.00	0.95 \pm 0.01	0.95 \pm 0.01
qsar	0.95 \pm 0.01	0.95 \pm 0.01	0.95 \pm 0.01	0.95 \pm 0.01	0.95 \pm 0.00	0.95 \pm 0.01	0.95 \pm 0.01
sulfur	0.95 \pm 0.01	0.95 \pm 0.01	0.95 \pm 0.01	0.95 \pm 0.00	0.95 \pm 0.01	0.95 \pm 0.01	0.95 \pm 0.01
superconductor	0.95 \pm 0.00	0.95 \pm 0.00	0.95 \pm 0.00	0.95 \pm 0.00	0.95 \pm 0.01	0.95 \pm 0.00	0.95 \pm 0.00

Table 7: Variant (a) NIW at 95% prediction intervals, aggregated across 10 seeds. Values ≥ 100 or < 0.01 are presented in scientific notation with 1 decimal place. **Bold** values (desirable) are the minimum for that dataset and metric, while the underlined values indicate the second-best result. **Red** values are more than 33% worse than the best result.

Dataset	CLEAR	ALEATORIC	ALEATORIC-R	PCS-EPISTEMIC	Naive	$\gamma_1 = 1$	$\lambda = 1$
aileron	0.193 \pm 0.016	0.208 \pm 0.017	0.195 \pm 0.017	0.215 \pm 0.016	0.220 \pm 0.021	<u>0.193 \pm 0.016</u>	0.193 \pm 0.016
airfoil	0.207 \pm 0.012	0.367 \pm 0.018	0.215 \pm 0.018	0.215 \pm 0.012	0.246 \pm 0.024	0.205 \pm 0.012	<u>0.206 \pm 0.012</u>
allstate	0.259 \pm 0.038	0.266 \pm 0.045	0.258 \pm 0.046	0.259 \pm 0.044	0.327 \pm 0.056	0.246 \pm 0.042	<u>0.247 \pm 0.042</u>
ca_housing	0.339 \pm 0.008	0.760 \pm 0.006	0.350 \pm 0.006	0.354 \pm 0.011	0.434 \pm 0.020	<u>0.333 \pm 0.006</u>	0.331 \pm 0.007
computer	0.091 \pm 0.008	0.099 \pm 0.001	0.092 \pm 0.010	18.269 \pm 11.847	0.115 \pm 0.007	0.091 \pm 0.010	0.091 \pm 0.007
concrete	0.249 \pm 0.025	0.486 \pm 0.028	0.265 \pm 0.029	0.249 \pm 0.017	0.263 \pm 0.028	0.251 \pm 0.022	0.253 \pm 0.023
elevator	0.156 \pm 0.009	0.144 \pm 0.007	0.149 \pm 0.007	0.178 \pm 0.012	0.144 \pm 0.008	0.156 \pm 0.009	0.160 \pm 0.008
energy_efficiency	0.047 \pm 0.005	0.212 \pm 0.015	0.050 \pm 0.007	0.062 \pm 0.006	0.062 \pm 0.013	0.051 \pm 0.004	0.053 \pm 0.004
insurance	0.313 \pm 0.033	0.329 \pm 0.042	0.328 \pm 0.058	0.585 \pm 0.167	0.478 \pm 0.070	0.332 \pm 0.079	0.298 \pm 0.047
kin8nm	0.360 \pm 0.012	0.490 \pm 0.020	0.374 \pm 0.014	0.373 \pm 0.014	0.397 \pm 0.017	0.359 \pm 0.012	0.360 \pm 0.011
miami_housing	0.085 \pm 0.002	0.105 \pm 0.001	0.086 \pm 0.004	0.098 \pm 0.003	0.126 \pm 0.006	0.084 \pm 0.002	0.085 \pm 0.002
naval_propulsion	6.1e-04 \pm 6.5e-06	6.2e-04 \pm 6.8e-06	6.0e-04 \pm 6.7e-06	7.2e-04 \pm 1.4e-05	6.0e-04 \pm 7.3e-06	6.2e-04 \pm 5.8e-06	6.1e-04 \pm 5.8e-06
parkinsons	0.227 \pm 0.010	0.321 \pm 0.013	0.250 \pm 0.014	0.312 \pm 0.021	0.303 \pm 0.022	0.228 \pm 0.008	0.225 \pm 0.009
powerplant	0.170 \pm 0.007	0.196 \pm 0.009	0.180 \pm 0.009	0.178 \pm 0.007	0.183 \pm 0.006	0.173 \pm 0.007	<u>0.172 \pm 0.007</u>
qsar	0.363 \pm 0.121	0.486 \pm 0.160	0.386 \pm 0.126	0.388 \pm 0.131	0.420 \pm 0.139	<u>0.362 \pm 0.121</u>	0.362 \pm 0.121
sulfur	0.109 \pm 0.011	0.112 \pm 0.010	0.107 \pm 0.010	0.131 \pm 0.017	0.122 \pm 0.015	<u>0.108 \pm 0.011</u>	0.108 \pm 0.011
superconductor	0.197 \pm 0.021	0.233 \pm 0.025	0.197 \pm 0.023	0.248 \pm 0.028	0.329 \pm 0.042	<u>0.195 \pm 0.021</u>	0.194 \pm 0.021

Table 8: Variant (a) QUANTILELOSS at 95% prediction intervals, aggregated across 10 seeds. Values ≥ 100 or < 0.01 are presented in scientific notation with 1 decimal place. **Bold** values (desirable) are the minimum for that dataset and metric, while the underlined values indicate the second-best result. **Red** values are more than 33% worse than the best result.

Dataset	CLEAR	ALEATORIC	ALEATORIC-R	PCS-EPISTEMIC	Naive	$\gamma_1 = 1$	$\lambda = 1$
aileron	9.2e-06 \pm 2.3e-07	1.0e-05 \pm 2.8e-07	9.7e-06 \pm 2.8e-07	1.0e-05 \pm 2.2e-07	1.1e-05 \pm 3.7e-07	<u>9.2e-06 \pm 2.3e-07</u>	9.2e-06 \pm 2.3e-07
airfoil	0.109 \pm 0.011	0.183 \pm 0.013	0.123 \pm 0.016	0.117 \pm 0.012	0.147 \pm 0.019	0.109 \pm 0.011	0.109 \pm 0.011
allstate	1.1e+02 \pm 7.627	1.3e+02 \pm 8.276	1.3e+02 \pm 7.950	1.2e+02 \pm 7.770	1.7e+02 \pm 13.696	1.1e+02 \pm 7.516	1.1e+02 \pm 7.566
ca_housing	2.8e+03 \pm 59.700	4.8e+03 \pm 25.753	3.0e+03 \pm 73.283	3.2e+03 \pm 93.396	4.0e+03 \pm 1.2e+02	<u>2.8e+03 \pm 66.414</u>	2.8e+03 \pm 70.545
computer	0.147 \pm 0.021	0.151 \pm 0.012	0.160 \pm 0.028	22.643 \pm 14.662	0.192 \pm 0.010	0.146 \pm 0.020	0.147 \pm 0.023
concrete	0.338 \pm 0.040	0.546 \pm 0.061	0.359 \pm 0.053	0.327 \pm 0.036	0.376 \pm 0.058	0.330 \pm 0.037	0.331 \pm 0.037
elevator	1.5e-04 \pm 2.0e-06	1.4e-04 \pm 2.9e-06	<u>1.5e-04 \pm 2.4e-06</u>	1.7e-04 \pm 5.6e-06	1.6e-04 \pm 5.1e-06	1.5e-04 \pm 2.4e-06	1.5e-04 \pm 2.0e-06
energy_efficiency	0.031 \pm 0.004	0.102 \pm 0.008	<u>0.033 \pm 0.005</u>	0.038 \pm 0.003	0.041 \pm 0.005	0.033 \pm 0.003	0.034 \pm 0.003
insurance	3.5e+02 \pm 57.411	3.7e+02 \pm 44.467	3.5e+02 \pm 51.063	5.8e+02 \pm 1.0e+02	4.4e+02 \pm 38.440	3.6e+02 \pm 67.343	3.5e+02 \pm 59.652
kin8nm	7.2e-03 \pm 1.7e-04	9.5e-03 \pm 1.6e-04	7.7e-03 \pm 2.7e-04	7.6e-03 \pm 9.7e-05	8.3e-03 \pm 2.5e-04	7.2e-03 \pm 1.6e-04	7.2e-03 \pm 1.7e-04
miami_housing	3.9e+03 \pm 1.9e+02	5.1e+03 \pm 3.1e+02	5.2e+03 \pm 3.4e+02	4.2e+03 \pm 1.6e+02	8.1e+03 \pm 3.6e+02	3.9e+03 \pm 1.9e+02	3.9e+03 \pm 1.8e+02
naval_propulsion	<u>1.5e-05 \pm 2.2e-07</u>	1.5e-05 \pm 2.7e-07	1.5e-05 \pm 2.8e-07	1.7e-05 \pm 2.8e-07	1.6e-05 \pm 3.5e-07	1.5e-05 \pm 2.2e-07	1.5e-05 \pm 2.4e-07
parkinsons	0.178 \pm 0.009	0.204 \pm 0.008	0.215 \pm 0.012	0.224 \pm 0.012	0.251 \pm 0.014	0.185 \pm 0.010	0.178 \pm 0.010
powerplant	0.212 \pm 0.012	0.228 \pm 0.011	0.220 \pm 0.011	0.221 \pm 0.012	0.231 \pm 0.010	0.213 \pm 0.012	0.213 \pm 0.012
qsar	0.049 \pm 0.003	0.060 \pm 0.003	0.052 \pm 0.003	0.053 \pm 0.003	0.057 \pm 0.003	0.049 \pm 0.003	0.049 \pm 0.003
sulfur	2.0e-03 \pm 1.3e-04	2.1e-03 \pm 1.2e-04	2.3e-03 \pm 1.1e-04	2.3e-03 \pm 1.9e-04	3.5e-03 \pm 2.0e-04	<u>2.0e-03 \pm 1.3e-04</u>	2.0e-03 \pm 1.3e-04
superconductor	<u>0.490 \pm 0.018</u>	0.512 \pm 0.015	0.539 \pm 0.024	0.608 \pm 0.023	0.861 \pm 0.036	0.490 \pm 0.018	0.491 \pm 0.018

Table 9: Variant (a) NCIW at 95% prediction intervals, aggregated across 10 seeds. Values ≥ 100 or < 0.01 are presented in scientific notation with 1 decimal place. **Bold** values (desirable) are the minimum for that dataset and metric, while the underlined values indicate the second-best result. **Red** values are more than 33% worse than the best result.

Dataset	CLEAR	ALEATORIC	ALEATORIC-R	PCS-EPISTEMIC	Naive	$\gamma_1 = 1$	$\lambda = 1$
aileron	0.195 \pm 0.017	0.209 \pm 0.019	0.196 \pm 0.017	0.217 \pm 0.021	0.220 \pm 0.020	0.195 \pm 0.017	0.195 \pm 0.017
airfoil	0.203 \pm 0.006	0.356 \pm 0.016	0.216 \pm 0.012	0.211 \pm 0.007	0.246 \pm 0.019	0.200 \pm 0.007	0.200 \pm 0.006
allstate	0.251 \pm 0.037	0.263 \pm 0.042	0.262 \pm 0.043	0.266 \pm 0.051	0.328 \pm 0.051	0.245 \pm 0.042	0.245 \pm 0.041
ca_housing	0.336 \pm 0.008	0.760 \pm 0.009	0.348 \pm 0.010	0.354 \pm 0.012	0.440 \pm 0.016	0.331 \pm 0.007	0.328 \pm 0.007
computer	0.091 \pm 0.008	0.099 \pm 0.001	0.092 \pm 0.011	0.112 \pm 0.028	0.113 \pm 0.008	0.092 \pm 0.009	0.091 \pm 0.007
concrete	0.246 \pm 0.033	0.421 \pm 0.079	0.259 \pm 0.035	0.241 \pm 0.025	0.264 \pm 0.037	0.238 \pm 0.027	0.240 \pm 0.026
elevator	0.155 \pm 0.010	0.143 \pm 0.008	0.148 \pm 0.008	0.177 \pm 0.011	0.145 \pm 0.010	0.155 \pm 0.010	0.159 \pm 0.010
energy_efficiency	0.046 \pm 0.005	0.196 \pm 0.032	0.050 \pm 0.005	0.057 \pm 0.004	0.060 \pm 0.006	0.050 \pm 0.005	0.051 \pm 0.004
insurance	0.306 \pm 0.032	0.281 \pm 0.049	0.307 \pm 0.045	0.530 \pm 0.178	0.454 \pm 0.102	0.283 \pm 0.049	0.270 \pm 0.045
kin8nm	0.354 \pm 0.008	0.482 \pm 0.014	0.371 \pm 0.009	0.371 \pm 0.009	0.396 \pm 0.013	0.355 \pm 0.008	0.355 \pm 0.008
miami_housing	<u>0.084 \pm 0.003</u>	0.106 \pm 0.004	0.085 \pm 0.003	0.098 \pm 0.002	0.124 \pm 0.006	0.083 \pm 0.002	0.084 \pm 0.002
naval_propulsion	6.1e-04 \pm 8.4e-06	6.1e-04 \pm 7.8e-06	<u>6.0e-04 \pm 5.6e-06</u>	7.1e-04 \pm 1.5e-05	6.0e-04 \pm 5.6e-06	6.1e-04 \pm 9.7e-06	6.1e-04 \pm 6.7e-06
parkinsons	0.226 \pm 0.010	0.321 \pm 0.013	0.248 \pm 0.008	0.316 \pm 0.032	0.302 \pm 0.013	0.228 \pm 0.007	0.225 \pm 0.009
powerplant	0.173 \pm 0.007	0.197 \pm 0.009	0.182 \pm 0.007	0.182 \pm 0.007	0.187 \pm 0.008	0.176 \pm 0.007	0.174 \pm 0.007
qsar	0.360 \pm 0.119	0.479 \pm 0.156	0.389 \pm 0.130	0.389 \pm 0.134	0.421 \pm 0.142	0.360 \pm 0.120	0.360 \pm 0.120
sulfur	0.109 \pm 0.010	0.111 \pm 0.009	0.107 \pm 0.009	0.128 \pm 0.013	0.129 \pm 0.011	0.108 \pm 0.011	0.107 \pm 0.011
superconductor	0.195 \pm 0.021	0.232 \pm 0.025	0.194 \pm 0.021	0.247 \pm 0.028	0.314 \pm 0.035	0.194 \pm 0.021	0.194 \pm 0.021

Table 10: Variant (a) INTERVALSCORELOSS at 95% prediction intervals, aggregated across 10 seeds. Values ≥ 100 or < 0.01 are presented in scientific notation with 1 decimal place. **Bold** values (desirable) are the minimum for that dataset and metric, while the underlined values indicate the second-best result. **Red** values are more than 33% worse than the best result.

Dataset	CLEAR	ALEATORIC	ALEATORIC-R	PCS-EPISTEMIC	Naive	$\gamma_1 = 1$	$\lambda = 1$
aileron	7.4e-04 \pm 1.8e-05	8.1e-04 \pm 2.2e-05	7.8e-04 \pm 2.2e-05	8.0e-04 \pm 1.8e-05	9.1e-04 \pm 2.9e-05	7.4e-04 \pm 1.8e-05	7.4e-04 \pm 1.8e-05
airfoil	8.717 \pm 0.870	14.669 \pm 1.007	9.843 \pm 1.249	9.397 \pm 0.977	11.761 \pm 1.548	8.727 \pm 0.902	8.730 \pm 0.892
allstate	9.1e+03 \pm 6.1e+02	1.1e+04 \pm 6.6e+02	1.0e+04 \pm 6.4e+02	9.9e+03 \pm 6.2e+02	1.3e+04 \pm 1.1e+03	9.2e+03 \pm 6.0e+02	9.2e+03 \pm 6.1e+02
ca_housing	2.2e+05 \pm 4.8e+03	3.9e+05 \pm 2.1e+03	2.4e+05 \pm 5.9e+03	2.6e+05 \pm 7.5e+03	3.2e+05 \pm 9.7e+03	2.2e+05 \pm 5.3e+03	2.2e+05 \pm 5.6e+03
computer	11.776 \pm 1.705	12.049 \pm 0.920	12.799 \pm 2.265	1.8e+03 \pm 1.2e+03	15.360 \pm 0.785	11.697 \pm 1.583	11.786 \pm 1.829
concrete	27.020 \pm 3.202	43.690 \pm 4.842	28.684 \pm 4.251	26.165 \pm 2.857	30.054 \pm 4.640	26.365 \pm 2.976	26.445 \pm 2.996
elevator	0.012 \pm 0.000	0.011 \pm 0.000	0.012 \pm 0.000	0.014 \pm 0.000	0.013 \pm 0.000	0.012 \pm 0.000	0.012 \pm 0.000
energy_efficiency	2.465 \pm 0.347	8.199 \pm 0.672	2.671 \pm 0.416	3.058 \pm 0.217	3.253 \pm 0.388	2.667 \pm 0.280	2.721 \pm 0.270
insurance	2.8e+04 \pm 4.6e+03	2.9e+04 \pm 3.6e+03	2.8e+04 \pm 4.1e+03	4.7e+04 \pm 8.1e+03	3.6e+04 \pm 3.1e+03	2.9e+04 \pm 5.4e+03	2.8e+04 \pm 4.8e+03
kin8nm	0.577 \pm 0.014	0.760 \pm 0.013	0.616 \pm 0.021	0.607 \pm 0.008	0.666 \pm 0.020	0.577 \pm 0.013	0.577 \pm 0.013
miami_housing	3.1e+05 \pm 1.5e+04	4.1e+05 \pm 2.5e+04	4.2e+05 \pm 2.7e+04	3.3e+05 \pm 1.3e+04	6.5e+05 \pm 2.9e+04	3.1e+05 \pm 1.5e+04	3.1e+05 \pm 1.5e+04
naval_propulsion	1.2e-03 \pm 1.8e-05	1.2e-03 \pm 2.2e-05	1.2e-03 \pm 2.2e-05	1.4e-03 \pm 2.3e-05	1.3e-03 \pm 2.8e-05	1.2e-03 \pm 1.8e-05	1.2e-03 \pm 1.9e-05
parkinsons	14.235 \pm 0.752	16.303 \pm 0.641	17.210 \pm 0.950	17.947 \pm 0.957	20.088 \pm 1.130	14.779 \pm 0.840	14.274 \pm 0.762
powerplant	16.993 \pm 0.937	18.211 \pm 0.897	17.577 \pm 0.884	17.715 \pm 0.965	18.501 \pm 0.815	17.064 \pm 0.951	17.027 \pm 0.954
qsar	3.951 \pm 0.230	4.795 \pm 0.219	4.187 \pm 0.231	4.249 \pm 0.217	4.558 \pm 0.216	3.950 \pm 0.225	3.953 \pm 0.224
sulfur	0.161 \pm 0.011	0.172 \pm 0.010	0.187 \pm 0.008	0.186 \pm 0.015	0.280 \pm 0.016	0.161 \pm 0.011	0.161 \pm 0.011
superconductor	<u>39.230 \pm 1.437</u>	40.925 \pm 1.177	43.103 \pm 1.911	48.630 \pm 1.867	68.891 \pm 2.882	39.196 \pm 1.455	39.314 \pm 1.475

E.2 Variant (b)

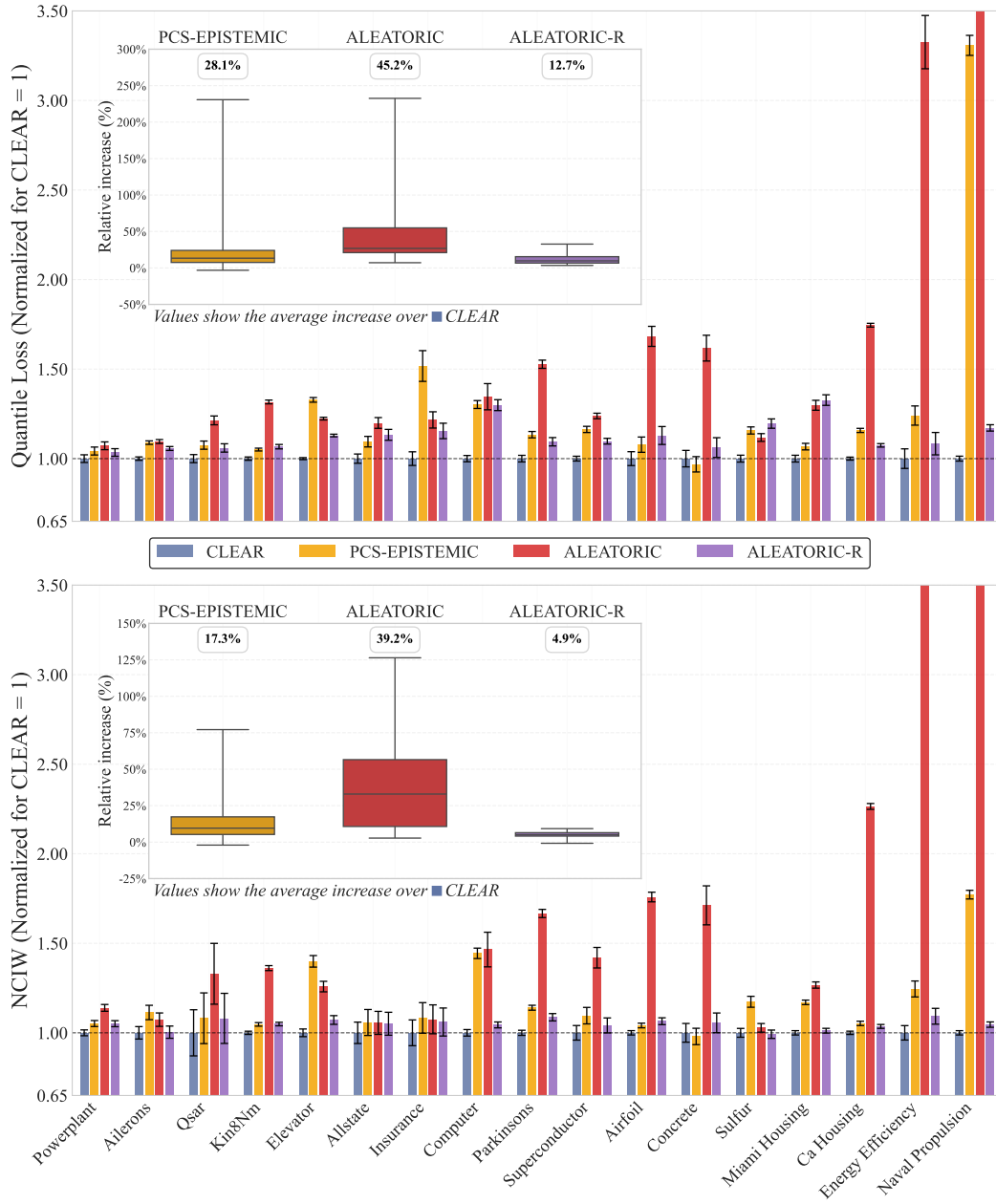


Figure 7: Quantile loss and NCIW performance of different methods (CLEAR, PCS, ALEATORIC, ALEATORIC-R) for variant (b), over 10 seeds normalized relative to CLEAR (baseline = 1.0). Lower values indicate better performance. The inset boxplot shows the % improvement relative to the CLEAR baseline $\pm 1\sigma$. Values inside each subplot represent the mean improvement across all datasets.

Table 11: Variant (b) PICP at 95% prediction intervals, aggregated across 10 seeds.

Dataset	CLEAR	ALEATORIC	ALEATORIC-R	PCS-EPISTEMIC	Naive	$\gamma_1 = 1$	$\lambda = 1$
ailérons	0.95 ± 0.00	0.95 ± 0.00	0.95 ± 0.00	0.95 ± 0.01	0.95 ± 0.01	0.95 ± 0.00	0.95 ± 0.00
airfoil	0.95 ± 0.01	0.95 ± 0.01	0.95 ± 0.01	0.95 ± 0.01	0.95 ± 0.02	0.95 ± 0.02	0.95 ± 0.01
allstate	0.95 ± 0.01	0.95 ± 0.01	0.95 ± 0.01	0.94 ± 0.01	0.95 ± 0.01	0.95 ± 0.01	0.95 ± 0.01
ca_housing	0.95 ± 0.01	0.95 ± 0.01	0.95 ± 0.01	0.95 ± 0.01	0.95 ± 0.01	0.95 ± 0.01	0.95 ± 0.01
computer	0.95 ± 0.01	0.95 ± 0.01	0.95 ± 0.01	0.95 ± 0.01	0.95 ± 0.01	0.95 ± 0.01	0.95 ± 0.01
concrete	0.95 ± 0.02	0.96 ± 0.02	0.95 ± 0.02	0.95 ± 0.01	0.94 ± 0.03	0.95 ± 0.01	0.95 ± 0.01
elevator	0.95 ± 0.00	0.95 ± 0.00	0.95 ± 0.01	0.95 ± 0.00	0.95 ± 0.01	0.95 ± 0.00	0.95 ± 0.00
energy_efficiency	0.95 ± 0.02	0.96 ± 0.02	0.95 ± 0.02	0.96 ± 0.01	0.95 ± 0.02	0.96 ± 0.01	0.96 ± 0.01
insurance	0.95 ± 0.01	0.96 ± 0.01	0.96 ± 0.02	0.95 ± 0.01	0.95 ± 0.02	0.96 ± 0.01	0.96 ± 0.01
kin8nm	0.95 ± 0.01	0.95 ± 0.01	0.95 ± 0.01	0.95 ± 0.01	0.95 ± 0.01	0.95 ± 0.01	0.95 ± 0.01
miami_housing	0.95 ± 0.01	0.95 ± 0.00	0.95 ± 0.01	0.95 ± 0.01	0.95 ± 0.01	0.95 ± 0.00	0.95 ± 0.00
naval_propulsion	0.95 ± 0.01	0.95 ± 0.00	0.95 ± 0.01	1.00 ± 0.00	0.95 ± 0.00	0.95 ± 0.01	0.95 ± 0.00
parkinsons	0.95 ± 0.01	0.95 ± 0.01	0.95 ± 0.01	0.95 ± 0.01	0.95 ± 0.01	0.95 ± 0.01	0.95 ± 0.01
powerplant	0.95 ± 0.01	0.95 ± 0.00	0.95 ± 0.01	0.95 ± 0.01	0.95 ± 0.00	0.95 ± 0.01	0.95 ± 0.01
qsar	0.95 ± 0.01	0.95 ± 0.01	0.95 ± 0.01	0.95 ± 0.01	0.95 ± 0.00	0.95 ± 0.01	0.95 ± 0.01
sulfur	0.95 ± 0.01	0.95 ± 0.01	0.95 ± 0.01	0.95 ± 0.00	0.95 ± 0.01	0.95 ± 0.01	0.95 ± 0.01
superconductor	0.95 ± 0.00	0.95 ± 0.01	0.95 ± 0.00	0.95 ± 0.00	0.95 ± 0.00	0.95 ± 0.00	0.95 ± 0.00

Table 12: Variant (b) NIW at 95% prediction intervals, aggregated across 10 seeds. Values ≥ 100 or < 0.01 are presented in scientific notation with 1 decimal place. **Bold** values (desirable) are the minimum for that dataset and metric, while the underlined values indicate the second-best result. **Red** values are more than 33% worse than the best result.

Dataset	CLEAR	ALEATORIC	ALEATORIC-R	PCS-EPISTEMIC	Naive	$\gamma_1 = 1$	$\lambda = 1$
ailérons	0.193 ± 0.016	0.208 ± 0.017	0.195 ± 0.017	0.215 ± 0.016	0.220 ± 0.021	0.193 ± 0.016	0.193 ± 0.016
airfoil	0.207 ± 0.012	0.367 ± 0.018	0.215 ± 0.018	0.215 ± 0.012	0.246 ± 0.024	0.205 ± 0.012	0.206 ± 0.012
allstate	0.256 ± 0.041	0.264 ± 0.047	0.258 ± 0.046	0.255 ± 0.048	0.326 ± 0.056	0.243 ± 0.045	0.244 ± 0.045
ca_housing	0.339 ± 0.008	0.760 ± 0.006	0.350 ± 0.006	0.354 ± 0.011	0.434 ± 0.020	0.333 ± 0.006	0.331 ± 0.007
computer	0.099 ± 0.006	0.143 ± 0.029	0.104 ± 0.005	0.142 ± 0.009	0.113 ± 0.006	<u>0.101 ± 0.005</u>	0.104 ± 0.005
concrete	0.249 ± 0.025	0.486 ± 0.028	0.265 ± 0.029	0.249 ± 0.017	0.263 ± 0.028	0.251 ± 0.022	0.253 ± 0.023
elevator	0.137 ± 0.007	0.171 ± 0.010	0.146 ± 0.008	0.193 ± 0.013	0.169 ± 0.010	0.136 ± 0.008	0.137 ± 0.008
energy_efficiency	0.047 ± 0.005	0.212 ± 0.015	0.050 ± 0.007	0.062 ± 0.006	0.062 ± 0.013	0.051 ± 0.004	0.053 ± 0.004
insurance	0.329 ± 0.045	0.407 ± 0.064	0.381 ± 0.055	0.434 ± 0.179	0.478 ± 0.070	0.339 ± 0.104	0.306 ± 0.058
kin8nm	0.360 ± 0.012	0.490 ± 0.020	0.374 ± 0.014	0.373 ± 0.014	0.397 ± 0.017	0.359 ± 0.012	0.360 ± 0.011
miami_housing	0.085 ± 0.002	0.105 ± 0.001	0.086 ± 0.004	0.098 ± 0.003	0.126 ± 0.006	0.084 ± 0.002	0.085 ± 0.002
naval_propulsion	1.9e-03 ± 7.3e-05	0.222 ± 0.003	1.9e-03 ± 9.7e-05	8.1e-03 ± 4.1e-04	2.4e-03 ± 1.4e-04	2.1e-03 ± 8.1e-05	2.8e-03 ± 1.3e-04
parkinsons	0.281 ± 0.009	0.483 ± 0.006	0.302 ± 0.012	0.325 ± 0.011	0.345 ± 0.011	0.282 ± 0.009	0.281 ± 0.009
powerplant	0.170 ± 0.007	0.196 ± 0.009	0.180 ± 0.009	0.178 ± 0.007	0.183 ± 0.006	0.173 ± 0.007	0.172 ± 0.007
qsar	0.363 ± 0.121	0.486 ± 0.160	0.386 ± 0.126	0.388 ± 0.131	0.420 ± 0.139	0.362 ± 0.121	0.362 ± 0.121
sulfur	0.108 ± 0.009	0.110 ± 0.008	0.107 ± 0.011	0.129 ± 0.014	0.122 ± 0.015	0.106 ± 0.009	0.106 ± 0.009
superconductor	<u>0.218 ± 0.023</u>	0.309 ± 0.033	0.229 ± 0.025	0.240 ± 0.026	0.354 ± 0.043	0.223 ± 0.024	0.215 ± 0.024

Table 13: Variant (b) QUANTILELOSS at 95% prediction intervals, aggregated across 10 seeds. Values ≥ 100 or < 0.01 are presented in scientific notation with 1 decimal place. **Bold** values (desirable) are the minimum for that dataset and metric, while the underlined values indicate the second-best result. **Red** values are more than 33% worse than the best result.

Dataset	CLEAR	ALEATORIC	ALEATORIC-R	PCS-EPISTEMIC	Naive	$\gamma_1 = 1$	$\lambda = 1$
ailérons	9.2e-06 ± 2.3e-07	1.0e-05 ± 2.8e-07	9.7e-06 ± 2.8e-07	1.0e-05 ± 2.2e-07	1.1e-05 ± 3.7e-07	9.2e-06 ± 2.3e-07	9.2e-06 ± 2.3e-07
airfoil	0.109 ± 0.011	0.183 ± 0.013	0.123 ± 0.016	0.117 ± 0.012	0.147 ± 0.019	0.109 ± 0.011	0.109 ± 0.011
allstate	1.1e+02 ± 7.568	1.4e+02 ± 8.571	1.3e+02 ± 9.257	1.2e+02 ± 9.008	1.7e+02 ± 11.065	1.2e+02 ± 8.331	1.1e+02 ± 8.358
ca_housing	2.8e+03 ± 59.700	4.8e+03 ± 25.753	3.0e+03 ± 73.283	3.2e+03 ± 93.396	4.0e+03 ± 1.2e+02	2.8e+03 ± 66.414	2.8e+03 ± 70.545
computer	0.159 ± 0.007	0.214 ± 0.041	0.206 ± 0.015	0.207 ± 0.009	0.234 ± 0.019	0.159 ± 0.007	0.161 ± 0.008
concrete	0.338 ± 0.040	0.546 ± 0.061	0.359 ± 0.053	0.327 ± 0.036	0.376 ± 0.058	0.330 ± 0.037	0.331 ± 0.037
elevator	1.4e-04 ± 2.0e-06	1.8e-04 ± 3.0e-06	1.6e-04 ± 3.1e-06	1.9e-04 ± 6.2e-06	2.1e-04 ± 5.5e-06	1.4e-04 ± 2.0e-06	1.4e-04 ± 2.1e-06
energy_efficiency	0.031 ± 0.004	0.102 ± 0.008	0.033 ± 0.005	0.038 ± 0.003	0.041 ± 0.005	0.033 ± 0.003	0.034 ± 0.003
insurance	3.2e+02 ± 31.593	3.9e+02 ± 36.904	3.7e+02 ± 35.107	4.9e+02 ± 88.647	4.4e+02 ± 34.159	3.7e+02 ± 62.380	3.4e+02 ± 40.487
kin8nm	7.2e-03 ± 1.7e-04	9.5e-03 ± 1.6e-04	7.7e-03 ± 2.7e-04	7.6e-03 ± 9.7e-05	8.3e-03 ± 2.5e-04	7.2e-03 ± 1.6e-04	7.2e-03 ± 1.7e-04
miami_housing	3.9e+03 ± 1.9e+02	5.1e+03 ± 3.1e+02	5.2e+03 ± 3.4e+02	4.2e+03 ± 1.6e+02	8.1e+03 ± 3.6e+02	3.9e+03 ± 1.9e+02	3.9e+03 ± 1.8e+02
naval_propulsion	5.4e-05 ± 1.9e-06	4.9e-03 ± 7.0e-05	6.4e-05 ± 2.7e-06	1.8e-04 ± 9.1e-06	8.8e-05 ± 5.9e-06	6.0e-05 ± 1.8e-06	7.5e-05 ± 2.7e-06
parkinsons	0.209 ± 0.010	0.319 ± 0.009	0.228 ± 0.014	0.237 ± 0.008	0.265 ± 0.013	0.209 ± 0.010	0.209 ± 0.009
powerplant	0.212 ± 0.012	0.228 ± 0.011	0.220 ± 0.011	0.221 ± 0.012	0.231 ± 0.010	0.213 ± 0.012	0.213 ± 0.012
qsar	0.049 ± 0.003	0.060 ± 0.003	0.052 ± 0.003	0.053 ± 0.003	0.057 ± 0.003	0.049 ± 0.003	0.049 ± 0.003
sulfur	1.9e-03 ± 9.6e-05	2.2e-03 ± 1.1e-04	2.3e-03 ± 1.4e-04	2.2e-03 ± 8.6e-05	3.5e-03 ± 2.4e-04	1.9e-03 ± 8.2e-05	1.9e-03 ± 8.6e-05
superconductor	<u>0.522 ± 0.018</u>	0.647 ± 0.019	0.573 ± 0.023	0.607 ± 0.025	0.891 ± 0.035	0.522 ± 0.018	0.522 ± 0.019

Table 14: Variant (b) NCIW at 95% prediction intervals, aggregated across 10 seeds. Values ≥ 100 or < 0.01 are presented in scientific notation with 1 decimal place. **Bold** values (desirable) are the minimum for that dataset and metric, while the underlined values indicate the second-best result. **Red** values are more than 33% worse than the best result.

Dataset	CLEAR	ALEATORIC	ALEATORIC-R	PCS-EPISTEMIC	Naive	$\gamma_1 = 1$	$\lambda = 1$
aileron	0.195 \pm 0.017	0.209 \pm 0.019	0.196 \pm 0.017	0.217 \pm 0.021	0.220 \pm 0.020	0.195 \pm 0.017	0.195 \pm 0.017
airfoil	0.203 \pm 0.006	0.356 \pm 0.016	0.216 \pm 0.012	0.211 \pm 0.007	0.246 \pm 0.019	0.200 \pm 0.007	0.200 \pm 0.006
allstate	0.250 \pm 0.039	0.264 \pm 0.042	0.262 \pm 0.042	0.264 \pm 0.052	0.325 \pm 0.053	0.244 \pm 0.043	0.244 \pm 0.042
ca_housing	0.336 \pm 0.008	0.760 \pm 0.009	0.348 \pm 0.010	0.354 \pm 0.012	0.440 \pm 0.016	0.331 \pm 0.007	0.328 \pm 0.007
computer	0.098 \pm 0.005	0.144 \pm 0.034	0.103 \pm 0.003	0.142 \pm 0.008	0.111 \pm 0.005	0.101 \pm 0.004	0.105 \pm 0.004
concrete	0.246 \pm 0.033	0.421 \pm 0.079	0.259 \pm 0.035	0.241 \pm 0.025	0.264 \pm 0.037	0.238 \pm 0.027	0.240 \pm 0.026
elevator	0.137 \pm 0.008	0.173 \pm 0.011	0.147 \pm 0.009	0.192 \pm 0.012	0.168 \pm 0.012	0.137 \pm 0.007	0.137 \pm 0.007
energy_efficiency	0.046 \pm 0.005	0.196 \pm 0.032	0.050 \pm 0.005	0.057 \pm 0.004	0.060 \pm 0.006	0.050 \pm 0.005	0.051 \pm 0.004
insurance	0.320 \pm 0.059	0.344 \pm 0.069	0.339 \pm 0.066	0.346 \pm 0.076	0.455 \pm 0.090	0.292 \pm 0.058	0.275 \pm 0.054
kin8nm	0.354 \pm 0.008	0.482 \pm 0.014	0.371 \pm 0.009	0.371 \pm 0.009	0.396 \pm 0.013	0.355 \pm 0.008	0.355 \pm 0.008
miami_housing	0.084 \pm 0.003	0.106 \pm 0.004	0.085 \pm 0.003	0.098 \pm 0.002	0.124 \pm 0.006	0.083 \pm 0.002	0.084 \pm 0.002
naval_propulsion	1.8e-03 \pm 5.6e-05	0.195 \pm 0.011	1.9e-03 \pm 8.0e-05	3.2e-03 \pm 1.2e-04	2.4e-03 \pm 1.4e-04	2.1e-03 \pm 7.2e-05	2.8e-03 \pm 1.1e-04
parkinsons	0.284 \pm 0.010	0.473 \pm 0.016	0.309 \pm 0.018	0.324 \pm 0.008	0.349 \pm 0.019	0.285 \pm 0.011	0.285 \pm 0.011
powerplant	0.173 \pm 0.007	0.197 \pm 0.009	0.182 \pm 0.007	0.182 \pm 0.007	0.187 \pm 0.008	0.176 \pm 0.007	0.174 \pm 0.007
qsar	0.360 \pm 0.119	0.479 \pm 0.156	0.389 \pm 0.130	0.389 \pm 0.134	0.421 \pm 0.142	0.360 \pm 0.120	0.360 \pm 0.120
sulfur	0.106 \pm 0.007	0.109 \pm 0.006	0.105 \pm 0.006	0.125 \pm 0.009	0.127 \pm 0.008	0.105 \pm 0.006	0.104 \pm 0.006
superconductor	0.217 \pm 0.023	0.308 \pm 0.032	0.226 \pm 0.023	0.238 \pm 0.026	0.347 \pm 0.037	0.222 \pm 0.023	0.215 \pm 0.023

Table 15: Variant (b) INTERVALSCORELOSS at 95% prediction intervals, aggregated across 10 seeds. Values ≥ 100 or < 0.01 are presented in scientific notation with 1 decimal place. **Bold** values (desirable) are the minimum for that dataset and metric, while the underlined values indicate the second-best result. **Red** values are more than 33% worse than the best result.

Dataset	CLEAR	ALEATORIC	ALEATORIC-R	PCS-EPISTEMIC	Naive	$\gamma_1 = 1$	$\lambda = 1$
aileron	7.4e-04 \pm 1.8e-05	8.1e-04 \pm 2.2e-05	7.8e-04 \pm 2.2e-05	8.0e-04 \pm 1.8e-05	9.1e-04 \pm 2.9e-05	7.4e-04 \pm 1.8e-05	7.4e-04 \pm 1.8e-05
airfoil	8.717 \pm 0.870	14.669 \pm 1.007	9.843 \pm 1.249	9.397 \pm 0.977	11.761 \pm 1.548	8.727 \pm 0.902	8.730 \pm 0.892
allstate	9.1e+03 \pm 6.1e+02	1.1e+04 \pm 6.9e+02	1.0e+04 \pm 7.4e+02	1.0e+04 \pm 7.2e+02	1.3e+04 \pm 8.9e+02	9.2e+03 \pm 6.7e+02	9.2e+03 \pm 6.7e+02
ca_housing	2.2e+05 \pm 4.8e+03	3.9e+05 \pm 2.1e+03	2.4e+05 \pm 5.9e+03	2.6e+05 \pm 7.5e+03	3.2e+05 \pm 9.7e+03	2.2e+05 \pm 5.3e+03	2.2e+05 \pm 5.6e+03
computer	12.707 \pm 0.575	17.102 \pm 3.298	16.503 \pm 1.199	16.547 \pm 0.692	18.684 \pm 1.517	12.707 \pm 0.591	12.897 \pm 0.602
concrete	27.020 \pm 3.202	43.690 \pm 4.842	28.684 \pm 4.251	26.165 \pm 2.857	30.054 \pm 4.640	26.365 \pm 2.976	26.445 \pm 2.996
elevator	0.011 \pm 0.000	0.014 \pm 0.000	0.013 \pm 0.000	0.015 \pm 0.000	0.017 \pm 0.000	0.012 \pm 0.000	0.012 \pm 0.000
energy_efficiency	2.465 \pm 0.347	8.199 \pm 0.672	2.671 \pm 0.416	3.058 \pm 0.217	3.253 \pm 0.388	2.667 \pm 0.280	2.721 \pm 0.270
insurance	2.6e+04 \pm 2.5e+03	3.1e+04 \pm 3.0e+03	3.0e+04 \pm 2.8e+03	3.9e+04 \pm 7.1e+03	3.5e+04 \pm 2.7e+03	3.0e+04 \pm 5.0e+03	2.8e+04 \pm 3.2e+03
kin8nm	0.577 \pm 0.014	0.760 \pm 0.013	0.616 \pm 0.021	0.607 \pm 0.008	0.666 \pm 0.020	0.577 \pm 0.013	0.577 \pm 0.013
miami_housing	3.1e+05 \pm 1.5e+04	4.1e+05 \pm 2.5e+04	4.2e+05 \pm 2.7e+04	3.3e+05 \pm 1.3e+04	6.5e+05 \pm 2.9e+04	3.1e+05 \pm 1.5e+04	3.1e+05 \pm 1.5e+04
naval_propulsion	4.4e-03 \pm 1.5e-04	0.391 \pm 0.006	5.1e-03 \pm 2.2e-04	0.014 \pm 0.001	7.1e-03 \pm 4.7e-04	4.8e-03 \pm 1.4e-04	6.0e-03 \pm 2.2e-04
parkinsons	16.697 \pm 0.794	25.497 \pm 0.692	18.270 \pm 1.122	18.931 \pm 0.600	21.220 \pm 1.011	16.688 \pm 0.771	16.680 \pm 0.750
powerplant	16.993 \pm 0.937	18.211 \pm 0.897	17.577 \pm 0.884	17.715 \pm 0.965	18.501 \pm 0.815	17.064 \pm 0.951	17.027 \pm 0.954
qsar	3.951 \pm 0.230	4.795 \pm 0.219	4.187 \pm 0.231	4.249 \pm 0.217	4.558 \pm 0.216	3.950 \pm 0.225	3.953 \pm 0.224
sulfur	0.155 \pm 0.008	0.174 \pm 0.009	0.186 \pm 0.012	0.180 \pm 0.007	0.277 \pm 0.020	0.156 \pm 0.007	0.155 \pm 0.007
superconductor	41.786 \pm 1.441	51.742 \pm 1.524	45.854 \pm 1.855	48.599 \pm 2.033	71.287 \pm 2.788	41.754 \pm 1.448	41.788 \pm 1.549

E.3 Variant (c)

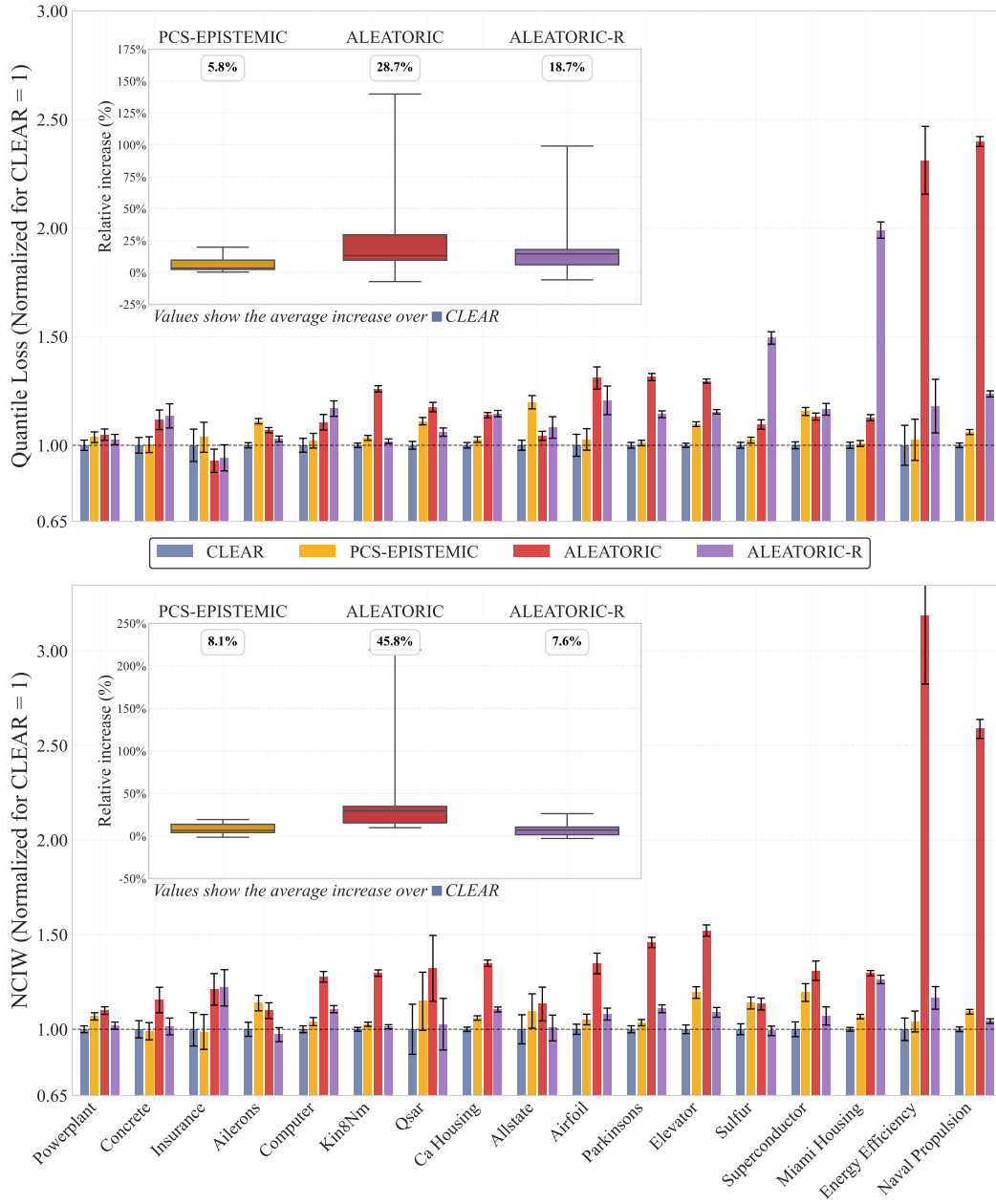


Figure 8: Quantile loss and NCIW performance of different methods (CLEAR, PCS, ALEATORIC, ALEATORIC-R) for variant (c), over 10 seeds normalized relative to CLEAR (baseline = 1.0). Lower values indicate better performance. The inset boxplot shows the % improvement relative to the CLEAR baseline $\pm 1\sigma$. Values inside each subplot represent the mean improvement across all datasets.

Table 16: Variant (c) PICP at 95% prediction intervals, aggregated across 10 seeds.

Dataset	CLEAR	ALEATORIC	ALEATORIC-R	PCS-EPISTEMIC	Naive	UACQR-P	UACQR-S
ailérons	0.95 ± 0.01	0.95 ± 0.01	0.95 ± 0.01	0.95 ± 0.01	0.95 ± 0.01	0.95 ± 0.01	0.96 ± 0.00
airfoil	0.96 ± 0.01	0.95 ± 0.02	0.96 ± 0.01	0.95 ± 0.02	0.95 ± 0.02	0.95 ± 0.01	0.96 ± 0.01
allstate	0.95 ± 0.01	0.95 ± 0.01	0.95 ± 0.01	0.95 ± 0.01	0.95 ± 0.01	0.95 ± 0.01	0.95 ± 0.01
ca_housing	0.95 ± 0.01	0.95 ± 0.01	0.95 ± 0.01	0.95 ± 0.01	0.95 ± 0.01	0.95 ± 0.00	0.96 ± 0.00
computer	0.95 ± 0.01	0.95 ± 0.01	0.95 ± 0.01	0.95 ± 0.01	0.95 ± 0.01	0.95 ± 0.01	0.97 ± 0.00
concrete	0.96 ± 0.01	0.96 ± 0.02	0.96 ± 0.02	0.96 ± 0.01	0.95 ± 0.02	0.96 ± 0.02	0.96 ± 0.02
elevator	0.95 ± 0.01	0.95 ± 0.00	0.95 ± 0.00	0.95 ± 0.00	0.95 ± 0.00	0.95 ± 0.01	0.97 ± 0.00
energy_efficiency	0.95 ± 0.01	0.96 ± 0.02	0.96 ± 0.01	0.96 ± 0.02	0.95 ± 0.01	0.97 ± 0.02	0.96 ± 0.02
insurance	0.95 ± 0.01	0.95 ± 0.01	0.96 ± 0.02	0.96 ± 0.01	0.95 ± 0.01	0.96 ± 0.01	0.96 ± 0.01
kin8nm	0.95 ± 0.01	0.95 ± 0.01	0.95 ± 0.01	0.95 ± 0.01	0.95 ± 0.01	0.95 ± 0.01	0.95 ± 0.01
miami_housing	0.95 ± 0.01	0.95 ± 0.01	0.95 ± 0.01	0.95 ± 0.00	0.95 ± 0.01	0.95 ± 0.01	0.95 ± 0.01
naval_propulsion	0.95 ± 0.01	0.95 ± 0.01	0.95 ± 0.01	0.95 ± 0.01	0.95 ± 0.00	0.95 ± 0.01	0.99 ± 0.00
parkinsons	0.95 ± 0.01	0.95 ± 0.01	0.95 ± 0.01	0.95 ± 0.01	0.95 ± 0.01	0.95 ± 0.01	0.97 ± 0.01
powerplant	0.95 ± 0.01	0.95 ± 0.01	0.95 ± 0.01	0.95 ± 0.01	0.95 ± 0.01	0.95 ± 0.01	0.95 ± 0.01
qsar	0.95 ± 0.01	0.95 ± 0.01	0.95 ± 0.01	0.95 ± 0.01	0.95 ± 0.01	0.96 ± 0.01	0.96 ± 0.01
sulfur	0.95 ± 0.01	0.95 ± 0.01	0.95 ± 0.01	0.95 ± 0.01	0.95 ± 0.01	0.95 ± 0.00	0.95 ± 0.01
superconductor	0.95 ± 0.00	0.95 ± 0.00	0.95 ± 0.01	0.95 ± 0.00	0.95 ± 0.00	0.95 ± 0.00	0.95 ± 0.01

Table 17: Variant (c) NIW at 95% prediction intervals, aggregated across 10 seeds. Values ≥ 100 or < 0.01 are presented in scientific notation with 1 decimal place. **Bold** values (desirable) are the minimum for that dataset and metric, while the underlined values indicate the second-best result. **Red** values are more than 33% worse than the best result.

Dataset	CLEAR	ALEATORIC	ALEATORIC-R	PCS-EPISTEMIC	Naive	UACQR-P	UACQR-S
ailérons	0.208 ± 0.016	0.227 ± 0.018	0.203 ± 0.017	0.237 ± 0.024	0.229 ± 0.020	0.177 ± 0.014	0.207 ± 0.017
airfoil	0.201 ± 0.014	0.284 ± 0.016	0.223 ± 0.024	0.204 ± 0.019	0.214 ± 0.024	0.365 ± 0.022	0.391 ± 0.029
allstate	0.278 ± 0.052	0.317 ± 0.065	0.276 ± 0.047	0.299 ± 0.065	0.315 ± 0.059	0.285 ± 0.051	0.305 ± 0.055
ca_housing	0.314 ± 0.010	0.426 ± 0.005	0.346 ± 0.013	0.332 ± 0.011	0.400 ± 0.016	0.366 ± 0.007	0.405 ± 0.007
computer	0.080 ± 0.004	0.103 ± 0.001	0.089 ± 0.004	<u>0.084 ± 0.004</u>	0.091 ± 0.006	0.084 ± 0.003	0.101 ± 0.001
concrete	0.278 ± 0.029	0.319 ± 0.023	0.283 ± 0.027	0.273 ± 0.031	0.276 ± 0.028	0.373 ± 0.025	0.403 ± 0.022
elevator	0.127 ± 0.008	0.192 ± 0.010	0.137 ± 0.008	0.152 ± 0.008	0.144 ± 0.010	0.158 ± 0.011	0.200 ± 0.010
energy_efficiency	0.043 ± 0.007	0.137 ± 0.007	0.051 ± 0.005	0.045 ± 0.007	0.049 ± 0.005	inf ± nan	0.162 ± 0.014
insurance	0.397 ± 0.092	0.420 ± 0.051	0.460 ± 0.051	0.395 ± 0.096	0.423 ± 0.083	0.305 ± 0.046	0.311 ± 0.033
kin8nm	0.324 ± 0.011	0.414 ± 0.018	0.331 ± 0.013	0.329 ± 0.011	0.344 ± 0.012	0.446 ± 0.018	0.460 ± 0.019
miami_housing	0.088 ± 0.001	0.112 ± 0.002	0.113 ± 0.008	<u>0.093 ± 0.002</u>	0.123 ± 0.008	0.104 ± 0.003	0.113 ± 0.002
naval_propulsion	1.6e-03 ± 3.0e-05	4.1e-03 ± 8.4e-05	<u>1.6e-03 ± 4.1e-05</u>	1.7e-03 ± 5.4e-05	1.8e-03 ± 3.9e-05	1.7e-03 ± 8.2e-05	3.6e-03 ± 8.5e-05
parkinsons	0.250 ± 0.007	0.373 ± 0.012	0.281 ± 0.011	0.260 ± 0.008	0.285 ± 0.010	0.269 ± 0.020	0.313 ± 0.018
powerplant	0.157 ± 0.007	0.176 ± 0.008	0.161 ± 0.008	0.169 ± 0.006	0.164 ± 0.007	0.193 ± 0.007	0.202 ± 0.009
qsar	0.345 ± 0.116	0.464 ± 0.153	<u>0.354 ± 0.117</u>	0.395 ± 0.135	0.385 ± 0.131	0.410 ± 0.135	0.452 ± 0.152
sulfur	0.111 ± 0.009	0.124 ± 0.010	0.109 ± 0.013	0.124 ± 0.009	0.114 ± 0.013	0.115 ± 0.012	0.126 ± 0.012
superconductor	0.194 ± 0.020	0.250 ± 0.025	<u>0.211 ± 0.030</u>	0.231 ± 0.025	0.308 ± 0.035	0.220 ± 0.022	0.232 ± 0.026

Table 18: Variant (c) QUANTILELOSS at 95% prediction intervals, aggregated across 10 seeds. Values ≥ 100 or < 0.01 are presented in scientific notation with 1 decimal place. **Bold** values (desirable) are the minimum for that dataset and metric, while the underlined values indicate the second-best result. **Red** values are more than 33% worse than the best result.

Dataset	CLEAR	ALEATORIC	ALEATORIC-R	PCS-EPISTEMIC	Naive	UACQR-P	UACQR-S
ailérons	9.6e-06 ± 3.0e-07	1.0e-05 ± 2.7e-07	<u>9.9e-06 ± 3.6e-07</u>	1.1e-05 ± 2.7e-07	1.2e-05 ± 3.7e-07	1.0e-05 ± 0.0e+00	1.0e-05 ± 0.0e+00
airfoil	0.107 ± 0.014	0.140 ± 0.008	0.129 ± 0.019	0.110 ± 0.013	0.130 ± 0.019	0.188 ± 0.013	0.200 ± 0.010
allstate	1.2e+02 ± 6.844	1.2e+02 ± 5.120	1.2e+02 ± 19.422	1.4e+02 ± 9.738	1.6e+02 ± 10.676	1.1e+02 ± 7.356	1.2e+02 ± 6.507
ca_housing	2.8e+03 ± 91.370	3.2e+03 ± 69.918	3.2e+03 ± 1.0e+02	<u>2.9e+03 ± 87.120</u>	3.6e+03 ± 1.2e+02	3.0e+03 ± 58.564	3.0e+03 ± 57.081
computer	0.137 ± 0.011	0.152 ± 0.013	0.160 ± 0.012	<u>0.140 ± 0.012</u>	0.164 ± 0.013	0.147 ± 0.006	0.151 ± 0.004
concrete	0.335 ± 0.031	0.374 ± 0.043	0.380 ± 0.058	<u>0.336 ± 0.032</u>	0.384 ± 0.056	0.413 ± 0.037	0.425 ± 0.022
elevator	1.3e-04 ± 3.2e-06	1.7e-04 ± 2.3e-06	1.5e-04 ± 3.3e-06	<u>1.4e-04 ± 3.7e-06</u>	1.6e-04 ± 3.1e-06	1.8e-04 ± 5.4e-06	1.9e-04 ± 4.9e-06
energy_efficiency	0.029 ± 0.007	0.068 ± 0.004	0.034 ± 0.010	<u>0.030 ± 0.007</u>	0.034 ± 0.010	inf ± nan	0.079 ± 0.006
insurance	4.2e+02 ± 80.635	3.9e+02 ± 33.700	4.0e+02 ± 52.178	4.4e+02 ± 65.348	4.1e+02 ± 41.712	3.4e+02 ± 46.073	3.3e+02 ± 34.606
kin8nm	6.7e-03 ± 1.8e-04	8.4e-03 ± 2.7e-04	6.8e-03 ± 1.9e-04	6.9e-03 ± 2.2e-04	7.4e-03 ± 2.8e-04	8.8e-03 ± 1.6e-04	9.0e-03 ± 1.6e-04
miami_housing	3.7e+03 ± 1.4e+02	4.1e+03 ± 1.1e+02	7.3e+03 ± 4.2e+02	<u>3.7e+03 ± 1.2e+02</u>	7.7e+03 ± 4.2e+02	4.3e+03 ± 1.3e+02	4.5e+03 ± 1.3e+02
naval_propulsion	4.0e-05 ± 1.1e-06	9.5e-05 ± 2.1e-06	4.9e-05 ± 1.6e-06	<u>4.2e-05 ± 1.2e-06</u>	5.7e-05 ± 1.2e-06	9.3e-05 ± 9.0e-06	8.1e-05 ± 3.0e-06
parkinsons	0.189 ± 0.006	0.249 ± 0.007	0.217 ± 0.008	0.191 ± 0.006	0.220 ± 0.008	0.180 ± 0.009	0.200 ± 0.010
powerplant	0.203 ± 0.012	0.213 ± 0.014	0.208 ± 0.012	0.211 ± 0.013	0.211 ± 0.012	0.226 ± 0.011	0.234 ± 0.010
qsar	0.048 ± 0.002	0.057 ± 0.003	<u>0.051 ± 0.002</u>	0.053 ± 0.002	0.055 ± 0.003	0.051 ± 0.003	0.054 ± 0.002
sulfur	1.8e-03 ± 6.2e-05	2.0e-03 ± 1.2e-04	2.7e-03 ± 1.6e-04	<u>1.8e-03 ± 6.2e-05</u>	2.9e-03 ± 1.7e-04	1.9e-03 ± 1.2e-04	2.0e-03 ± 1.5e-04
superconductor	0.488 ± 0.020	0.553 ± 0.018	0.569 ± 0.042	<u>0.564 ± 0.023</u>	0.792 ± 0.035	<u>0.507 ± 0.017</u>	0.527 ± 0.016

Table 19: Variant (c) NCIW at 95% prediction intervals, aggregated across 10 seeds. Values ≥ 100 or < 0.01 are presented in scientific notation with 1 decimal place. **Bold** values (desirable) are the minimum for that dataset and metric, while the underlined values indicate the second-best result. **Red** values are more than 33% worse than the best result.

Dataset	CLEAR	ALEATORIC	ALEATORIC-R	PCS-EPISTEMIC	Naive	UACQR-P	UACQR-S
aileron	0.210 \pm 0.020	0.231 \pm 0.023	0.204 \pm 0.021	0.239 \pm 0.021	0.230 \pm 0.021	0.188 \pm 0.030	0.207 \pm 0.017
airfoil	0.189 \pm 0.013	0.255 \pm 0.033	0.204 \pm 0.016	0.199 \pm 0.013	0.204 \pm 0.014	0.317 \pm 0.025	0.329 \pm 0.033
allstate	0.278 \pm 0.055	0.315 \pm 0.066	0.280 \pm 0.041	0.305 \pm 0.070	0.319 \pm 0.051	0.279 \pm 0.047	0.296 \pm 0.049
ca_housing	0.310 \pm 0.009	0.418 \pm 0.015	0.343 \pm 0.011	0.329 \pm 0.009	0.401 \pm 0.018	0.368 \pm 0.007	0.405 \pm 0.007
computer	0.081 \pm 0.004	0.104 \pm 0.007	0.090 \pm 0.004	0.084 \pm 0.005	0.092 \pm 0.005	0.087 \pm 0.005	0.101 \pm 0.001
concrete	0.259 \pm 0.030	0.299 \pm 0.053	0.263 \pm 0.028	0.257 \pm 0.031	0.265 \pm 0.027	0.332 \pm 0.056	0.344 \pm 0.054
elevator	0.127 \pm 0.007	0.193 \pm 0.008	0.138 \pm 0.009	0.151 \pm 0.011	0.144 \pm 0.010	0.165 \pm 0.015	0.200 \pm 0.010
energy_efficiency	0.042 \pm 0.006	0.133 \pm 0.051	0.049 \pm 0.005	0.043 \pm 0.005	0.049 \pm 0.005	0.140 \pm 0.014	0.138 \pm 0.024
insurance	0.348 \pm 0.079	0.421 \pm 0.044	0.424 \pm 0.074	0.343 \pm 0.087	0.385 \pm 0.112	0.291 \pm 0.043	0.301 \pm 0.034
kin8nm	0.322 \pm 0.008	0.418 \pm 0.017	0.327 \pm 0.010	0.331 \pm 0.010	0.341 \pm 0.012	0.433 \pm 0.009	0.445 \pm 0.013
miami_housing	0.088 \pm 0.002	0.114 \pm 0.003	0.111 \pm 0.007	0.094 \pm 0.003	0.122 \pm 0.007	0.102 \pm 0.004	0.110 \pm 0.004
naval_propulsion	1.6e-03 \pm 4.9e-05	4.1e-03 \pm 2.6e-04	1.6e-03 \pm 4.8e-05	1.7e-03 \pm 4.7e-05	1.8e-03 \pm 5.8e-05	1.7e-03 \pm 8.2e-05	3.6e-03 \pm 8.5e-05
parkinsons	0.251 \pm 0.012	0.366 \pm 0.017	0.278 \pm 0.013	0.259 \pm 0.009	0.284 \pm 0.013	0.273 \pm 0.019	0.313 \pm 0.018
powerplant	0.160 \pm 0.007	0.176 \pm 0.008	0.164 \pm 0.008	0.171 \pm 0.008	0.166 \pm 0.007	0.191 \pm 0.009	0.200 \pm 0.009
qsar	0.349 \pm 0.119	0.461 \pm 0.155	0.358 \pm 0.123	0.400 \pm 0.139	0.393 \pm 0.132	0.409 \pm 0.134	0.449 \pm 0.150
sulfur	0.109 \pm 0.008	0.124 \pm 0.008	0.108 \pm 0.006	0.124 \pm 0.008	0.115 \pm 0.007	0.114 \pm 0.010	0.126 \pm 0.010
superconductor	0.192 \pm 0.019	0.252 \pm 0.026	0.206 \pm 0.027	0.230 \pm 0.023	0.297 \pm 0.030	0.220 \pm 0.023	0.232 \pm 0.025

Table 20: Variant (c) INTERVALSCORELOSS at 95% prediction intervals, aggregated across 10 seeds. Values ≥ 100 or < 0.01 are presented in scientific notation with 1 decimal place. **Bold** values (desirable) are the minimum for that dataset and metric, while the underlined values indicate the second-best result. **Red** values are more than 33% worse than the best result.

Dataset	CLEAR	ALEATORIC	ALEATORIC-R	PCS-EPISTEMIC	Naive	UACQR-P	UACQR-S
aileron	7.7e-04 \pm 2.4e-05	8.2e-04 \pm 2.2e-05	7.9e-04 \pm 2.9e-05	8.5e-04 \pm 2.2e-05	9.4e-04 \pm 3.0e-05	7.9e-04 \pm 3.1e-05	7.9e-04 \pm 2.3e-05
airfoil	8.567 \pm 1.121	11.223 \pm 0.608	10.339 \pm 1.545	8.799 \pm 1.034	10.361 \pm 1.499	15.052 \pm 1.025	15.999 \pm 0.776
allstate	9.2e+03 \pm 5.5e+02	9.6e+03 \pm 4.1e+02	1.0e+04 \pm 1.6e+03	1.1e+04 \pm 7.8e+02	1.3e+04 \pm 8.5e+02	9.0e+03 \pm 5.9e+02	9.3e+03 \pm 5.2e+02
ca_housing	2.2e+05 \pm 7.3e+03	2.5e+05 \pm 5.6e+03	2.5e+05 \pm 8.4e+03	2.3e+05 \pm 7.0e+03	2.9e+05 \pm 9.7e+03	2.4e+05 \pm 4.7e+03	2.4e+05 \pm 4.6e+03
computer	10.973 \pm 0.906	12.139 \pm 1.009	12.826 \pm 0.947	11.204 \pm 0.996	13.130 \pm 1.051	11.757 \pm 0.463	12.103 \pm 0.323
concrete	26.775 \pm 2.471	29.923 \pm 3.423	30.402 \pm 4.655	26.855 \pm 2.535	30.720 \pm 4.505	33.077 \pm 2.941	33.990 \pm 1.797
elevator	0.010 \pm 0.000	0.014 \pm 0.000	0.012 \pm 0.000	0.011 \pm 0.000	0.013 \pm 0.000	0.014 \pm 0.000	0.015 \pm 0.000
energy_efficiency	2.338 \pm 0.553	5.406 \pm 0.356	2.760 \pm 0.823	2.397 \pm 0.573	2.756 \pm 0.822	6.214 \pm 0.408	6.354 \pm 0.480
insurance	3.4e+04 \pm 6.5e+03	3.1e+04 \pm 2.7e+03	3.2e+04 \pm 4.2e+03	3.5e+04 \pm 5.2e+03	3.3e+04 \pm 3.3e+03	2.7e+04 \pm 3.7e+03	2.7e+04 \pm 2.8e+03
kin8nm	0.534 \pm 0.014	0.673 \pm 0.021	0.544 \pm 0.015	0.552 \pm 0.017	0.591 \pm 0.022	0.705 \pm 0.013	0.723 \pm 0.013
miami_housing	2.9e+05 \pm 1.1e+04	3.3e+05 \pm 8.9e+03	5.9e+05 \pm 3.4e+04	3.0e+05 \pm 9.6e+03	6.1e+05 \pm 3.4e+04	3.5e+05 \pm 1.0e+04	3.6e+05 \pm 1.0e+04
naval_propulsion	3.2e-03 \pm 8.6e-05	7.6e-03 \pm 1.6e-04	3.9e-03 \pm 1.2e-04	3.4e-03 \pm 9.6e-05	4.6e-03 \pm 9.6e-05	7.5e-03 \pm 7.5e-04	6.6e-03 \pm 1.3e-04
parkinsons	15.156 \pm 0.516	19.920 \pm 0.599	17.322 \pm 0.628	15.312 \pm 0.459	17.596 \pm 0.621	14.384 \pm 0.700	15.978 \pm 0.779
powerplant	16.242 \pm 0.989	17.038 \pm 1.138	16.671 \pm 0.987	16.846 \pm 1.029	16.874 \pm 0.975	18.078 \pm 0.906	18.725 \pm 0.822
qsar	3.850 \pm 0.177	4.528 \pm 0.221	4.083 \pm 0.194	4.278 \pm 0.129	4.392 \pm 0.203	4.102 \pm 0.230	4.333 \pm 0.182
sulfur	0.143 \pm 0.005	0.156 \pm 0.010	0.213 \pm 0.013	0.146 \pm 0.005	0.228 \pm 0.013	0.153 \pm 0.010	0.158 \pm 0.012
superconductor	39.048 \pm 1.591	44.219 \pm 1.421	45.523 \pm 3.375	45.127 \pm 1.849	63.336 \pm 2.769	40.545 \pm 1.386	42.122 \pm 1.257

Table 21: Variant (c) CLEAR calibration parameters λ and γ_1 for 95% prediction intervals across 10 seeds. Using all available variables. Showing median [min:max] values.

Dataset	λ	γ_1
aileron	1.05 [0.14:3.46]	0.98 [0.89:1.58]
airfoil	0.76 [0.16:5.93]	1.72 [0.22:4.56]
allstate	0.23 [0.00:15.89]	1.11 [0.15:1.94]
ca_housing	1.83 [1.01:3.70]	0.72 [0.42:0.98]
computer	2.29 [1.61:8.91]	0.73 [0.21:0.95]
concrete	1.95 [0.06:100.00]	0.84 [0.01:16.28]
elevator	0.95 [0.64:1.39]	1.03 [0.84:1.24]
energy_efficiency	0.12 [0.01:100.00]	7.27 [0.02:22.89]
insurance	5.06 [0.14:100.00]	0.38 [0.02:28.07]
kin8nm	1.98 [0.81:4.96]	0.75 [0.50:0.94]
miami_housing	6.88 [3.92:20.81]	0.24 [0.09:0.40]
naval_propulsion	16.32 [12.50:21.65]	0.64 [0.52:0.76]
parkinsons	1.18 [0.68:8.82]	1.26 [0.21:1.91]
powerplant	1.08 [0.82:3.62]	1.07 [0.47:1.27]
qsar	0.73 [0.41:1.32]	1.36 [1.04:2.13]
sulfur	2.49 [1.53:8.08]	0.69 [0.26:0.91]
superconductor	0.84 [0.37:1.79]	1.09 [0.69:1.30]

E.4 Comparing all variants of CLEAR

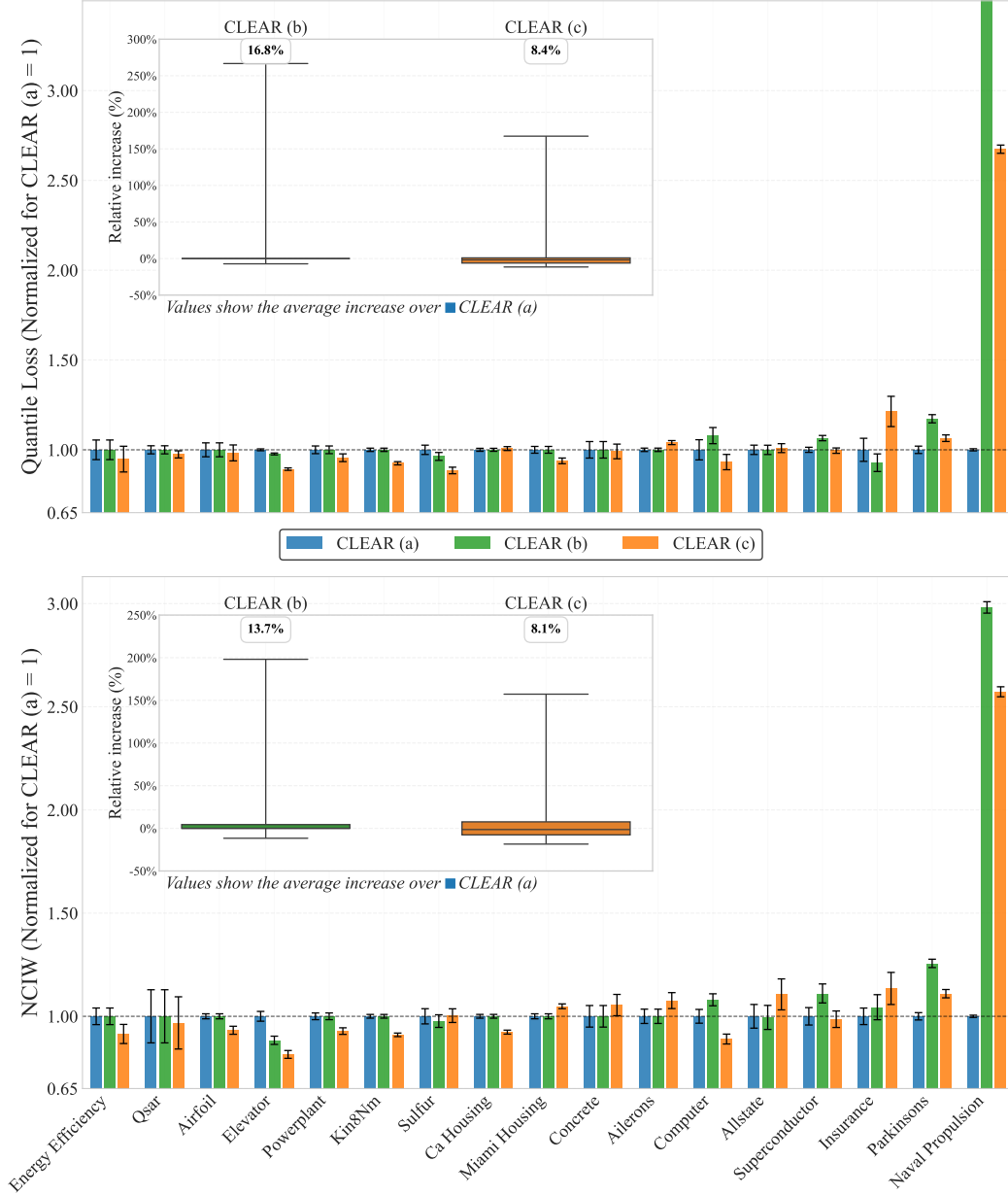


Figure 9: Quantile loss and NCIW performance of different variants of CLEAR (a, b and c) over 10 seeds normalized relative to CLEAR (a) (baseline = 1.0). Lower values indicate better performance. The inset boxplot shows the % improvement relative to the CLEAR (a) baseline $\pm 1\sigma$. Values inside each subplot represent the mean improvement across all datasets.

F Case Study: Housing Market Price Prediction and changing the number of predictors

We illustrate our method using the Ames Housing dataset, which contains data on 2,930 residential properties sold in Ames, Iowa, between 2006 and 2010. The target variable is the sale price of a house, and the full dataset includes around 80 predictor variables describing various aspects such as square footage, neighborhood, and building type. This dataset, originally collected by the Ames City Assessor’s Office and curated by [103], was explored in detail in Chapter 13 of [24].

The PCS framework [24] involves quantifying all sources of extended epistemic uncertainty stemming from the entire data-science cycle, such as uncertainty stemming from data processing. An pipeline of PCS uncertainty quantification applied to the Ames Housing data can be found in Chapter 13 in [24]. We follow the same steps³ for estimating \hat{f} and estimating epistemic uncertainty bounds $\hat{q}_{0.05}^{\text{epi}}, \hat{q}_{0.95}^{\text{epi}}$.

To investigate how the amount of available information affects predictive uncertainty, we consider two versions of the dataset:

- **Full:** the original dataset with all ~ 80 variables,
- **Top 2:** a further reduced dataset containing only the top two features (as determined by either feature importance of a random forest, or by correlation with the outcome variable, as both approaches lead to the same choice).

These settings simulate scenarios where fewer variables are available, reflecting different levels of information accessibility. Reducing the number of predictors is expected to increase aleatoric uncertainty (due to missing key predictive information) and decrease epistemic uncertainty (due to a simpler model class and lower dimensionality).

In each case, we applied the CLEAR procedure as described in Section 2.4. This involved: (1) data cleaning and preprocessing (excluding irregular sales, imputing missing values, encoding categorical variables), resulting in $N_1 = 438$ cleaned datasets; (2) fitting a predictive model \hat{f} and estimating epistemic uncertainty bounds $\hat{q}_{0.05}^{\text{epi}}, \hat{q}_{0.95}^{\text{epi}}$; (3) estimating aleatoric uncertainty bounds $\hat{q}_{0.05}^{\text{ale}}, \hat{q}_{0.95}^{\text{ale}}$ via quantile regression, as described in Section 2.3; (4) estimating λ and calibrating prediction intervals on the validation set.

Table 1 and the discussion in Section 4.3 summarize the results. In the reduced 2-variable setting, CLEAR selected $\lambda = 0.6$, assigning more weight to aleatoric uncertainty. In contrast, in the full-feature setting, $\lambda = 14.5$, emphasizing epistemic uncertainty. The corresponding calibrated epistemic-to-aleatoric ratios were computed as $\frac{1}{n} \sum_{i=1}^n \frac{\gamma_1 \times \text{epistemic}(x_i)}{\gamma_2 \times \text{aleatoric}(x_i)}$ in (1), reflecting the final width contributions from each component. They were 0.03 and 7.72, respectively. This ratio quantifies how much of the interval width is attributed to epistemic versus aleatoric uncertainty after calibration. The results demonstrate CLEAR’s ability to adaptively reweight the two uncertainty sources in response to the underlying information regime, producing intervals that are both sharp and well-calibrated across heterogeneous settings.

³Minor differences arise due to: (a) implementation differences in base models between R and Python, and (b) manual calibration of PCS intervals, which was not part of the original implementation. Additionally, both CQR and CLEAR were trained using only linear quantile regressors as the model selection step of PCS selected a linear model based on the RMSE on the validation dataset.

G Theory: coverage guarantees for CLEAR

G.1 Finite-sample marginal coverage for CLEAR

While conformal methods typically offer finite-sample marginal coverage guarantees, our implementation of CLEAR does not strictly adhere to these guarantees for two reasons:

1. We reuse the validation dataset \mathcal{D}_{val} as the calibration dataset, i.e., $\mathcal{D}_{\text{cal}} = \mathcal{D}_{\text{val}}$.
2. We optimize two parameters γ_1 and λ on the calibration dataset \mathcal{D}_{cal} .

However, our empirical results in Tables 6, 11 and 16 show that for reasonably sized datasets, this theoretical discrepancy does not visibly impact our practical marginal coverage. From a theoretical perspective, CLEAR still achieves asymptotic marginal coverage (as a consequence of asymptotic conditional coverage, see Lemma 2.1).

By slightly modifying the CLEAR procedure, we can obtain a theoretical finite-sample guarantee for marginal coverage under the standard exchangeability assumption, as in conformal inference, without sacrificing asymptotic conditional coverage. The key idea is to optimize the parameter λ using only a validation dataset \mathcal{D}_{val} , and then calibrate γ_1 using a separate, previously unseen calibration dataset \mathcal{D}_{cal} .

Definition G.1 (Conformalized CLEAR). Let the available data be split into a training set $\mathcal{D}_{\text{train}}$ and an old validation set $\mathcal{D}_{\text{val}}^{\text{old}}$. We first split $\mathcal{D}_{\text{val}}^{\text{old}}$ into two disjoint sets: a new validation set \mathcal{D}_{val} and a calibration set \mathcal{D}_{cal} . The procedure is as follows:

1. **Train and Optimize λ by running Algorithm 1 on $\mathcal{D}_{\text{train}}$ and \mathcal{D}_{val} :** The model \hat{f} and the uncertainty estimators are trained on $\mathcal{D}_{\text{train}}$ (Step 2 and 3 of Algorithm 1). The optimal value λ^* is found by optimizing the QuantileLoss on \mathcal{D}_{val} , without using any data from \mathcal{D}_{cal} (Step 4 and 5 of Algorithm 1).
2. **Compute Conformity Scores:** For each data point $(X_i, Y_i) \in \mathcal{D}_{\text{cal}}$, compute the conformity score $S_i^{\lambda^*}$:

$$S_i^{\lambda^*} = \max \left\{ \frac{\tilde{l}_{\lambda^*}(X_i) - Y_i}{\hat{f}(X_i) - \tilde{l}_{\lambda^*}(X_i)}, \frac{Y_i - \tilde{u}_{\lambda^*}(X_i)}{\tilde{u}_{\lambda^*}(X_i) - \hat{f}(X_i)} \right\}$$

where $\tilde{l}_{\lambda^*} := \hat{f} - \hat{q}_{\alpha/2}^{\text{ale}} - \lambda^* \hat{q}_{\alpha/2}^{\text{epi}}$ and $\tilde{u}_{\lambda^*} := \hat{f} + \hat{q}_{1-\alpha/2}^{\text{ale}} + \lambda^* \hat{q}_{1-\alpha/2}^{\text{epi}}$.

3. **Calibrate the Prediction Interval:** Set the calibration parameter γ_1^* to be the $\lceil (1 - \alpha)(|\mathcal{D}_{\text{cal}}| + 1) \rceil$ -th smallest value among the conformity scores $S_i^{\lambda^*}$ from \mathcal{D}_{cal} . If $\lceil (1 - \alpha)(|\mathcal{D}_{\text{cal}}| + 1) \rceil > |\mathcal{D}_{\text{cal}}|$, set $\gamma_1^* = \infty$.
4. **Form the Final Prediction Interval:** For a new test point x_{new} , the final $(1 - \alpha)$ -prediction interval is given by:

$$C(x_{\text{new}}) = \left[\hat{f}(x_{\text{new}}) - \gamma_1^* \left(\hat{q}_{\alpha/2}^{\text{ale}} + \lambda^* \hat{q}_{\alpha/2}^{\text{epi}} \right), \hat{f}(x_{\text{new}}) + \gamma_1^* \left(\hat{q}_{1-\alpha/2}^{\text{ale}} + \lambda^* \hat{q}_{1-\alpha/2}^{\text{epi}} \right) \right]$$

This modified version of CLEAR, which we call Conformalized CLEAR, satisfies the standard finite-sample marginal coverage guarantee of conformal prediction.

Lemma G.2. *Under the assumption that the data points in the calibration set \mathcal{D}_{cal} and the test point $(X_{\text{new}}, Y_{\text{new}})$ are exchangeable, the prediction interval $C(X_{\text{new}})$ generated by the Conformalized CLEAR procedure satisfies:*

$$\mathbb{P}(Y_{\text{new}} \in C(X_{\text{new}})) \geq 1 - \alpha.$$

Proof. The proof is a direct application of the standard theoretical guarantees for split conformal prediction. Since λ^* is determined using only data from \mathcal{D}_{val} , it is fixed with respect to the calibration set \mathcal{D}_{cal} . The conformity scores $S_i^{\lambda^*}$ are therefore exchangeable for all $(X_i, Y_i) \in \mathcal{D}_{\text{cal}} \cup \{(X_{\text{new}}, Y_{\text{new}})\}$. The choice of γ_1^* as the empirical $(1 - \alpha)(1 + 1/|\mathcal{D}_{\text{cal}}|)$ -quantile of the calibration scores ensures that the resulting prediction interval achieves at least $1 - \alpha$ marginal coverage, as established by [8, Theorem 1.4]. \square

However, in practice, we recommend using our default implementation of CLEAR, where the validation data is reused for calibration ($\mathcal{D}_{\text{cal}} = \mathcal{D}_{\text{val}}$). This improves data efficiency while still achieving strong approximate marginal coverage in our experiments (see Tables 6, 11 and 16). Avoiding a split allows more data for both validation and calibration, which improves model selection and stabilizes marginal and conditional coverage. Even when marginal coverage $\mathbb{P}(Y_{\text{new}} \in C(X_{\text{new}})) \geq 1 - \alpha$ is satisfied, the actual coverage $\mathbb{P}(Y_{\text{new}} \in C(X_{\text{new}}) | \mathcal{D}_{\text{train}}, \mathcal{D}_{\text{val}}, \mathcal{D}_{\text{cal}})$ can be significantly lower than the target coverage $1 - \alpha$ for a fixed calibration dataset \mathcal{D}_{cal} , due to the inherent variation of \mathcal{D}_{cal} . Only with sufficiently large calibration datasets \mathcal{D}_{cal} can we expect $\mathbb{P}(Y_{\text{new}} \in C(X_{\text{new}}) | \mathcal{D}_{\text{train}}, \mathcal{D}_{\text{val}}, \mathcal{D}_{\text{cal}})$ to be reliably close to $\mathbb{P}(Y_{\text{new}} \in C(X_{\text{new}}))$.⁴

G.2 Asymptotic conditional coverage for CLEAR — discussion of the assumptions in Lemma 2.1

The assumptions underlying Lemma 2.1 are generally mild and often satisfied in practice. The assumption that Λ is compact is particularly mild. In our experiments, we use a finite grid; for example, a combination of linearly spaced values from 0 to 0.09 and logarithmically spaced values from 0.1 to 100, resulting in approximately 4010 points. Intuitively, we believe that even if Λ were unbounded, the result of Lemma 2.1 would still hold, since QuantileLoss is a strictly proper scoring rule and thus would not lead to excessively large values of λ^* in the limit.

Lemma 2.1 also assumes consistency of the estimators. Many estimators satisfy this condition for both regression and quantile regression tasks:

1. Quantile Random Forests have been shown to consistently estimate quantiles under reasonable conditions, such as by regularizing the minimum number of samples per leaf [34]. Similarly, classical Random Forests are known to be consistent under standard assumptions [104]. Both QRF and Random Forests are available in our implementation of CLEAR.
2. Boosting methods trained on general loss functions can be made consistent under certain conditions, especially when regularized through early stopping [105]. This suggests that XGBoost and its quantile version, QXGB, can be consistent for suitable choices of hyperparameters. Both are included in our implementation of CLEAR.
3. More generally, regularized minimization of QuantileLoss over a sufficiently expressive function class on $\mathcal{D}_{\text{train}}$ yields consistent quantile estimators under broad assumptions [106].

In our experiments, we set $k = 1$, so Lemma 2.1 requires only one of the base models to be consistent.

Finally, note that Lemma 2.1 implicitly assumes i.i.d. data, as described in Section 2.1. For real-world datasets, this i.i.d. assumption is often the most difficult to justify in practice and may pose a greater challenge than the other assumptions in the lemma.

⁴Conformal theory provides theoretical guarantees for $\mathbb{P}(Y_{\text{new}} \in C(X_{\text{new}})) \geq 1 - \alpha$ and $\mathbb{P}(Y_{\text{new}} \in C(X_{\text{new}}) | \mathcal{D}_{\text{train}}, \mathcal{D}_{\text{val}}) \geq 1 - \alpha$ under the standard exchangeability assumption. However, it does *not* provide finite-sample guarantees for $\mathbb{P}(Y_{\text{new}} \in C(X_{\text{new}}) | \mathcal{D}_{\text{train}}, \mathcal{D}_{\text{val}}, \mathcal{D}_{\text{cal}})$ and $\mathbb{P}(Y_{\text{new}} \in C(X_{\text{new}}) | \mathcal{D}_{\text{cal}})$ for a fixed calibration dataset, even under the standard exchangeability assumption.

H On the Role of Relative and Absolute Uncertainty in Coverage Guarantees

In predictive inference, a fundamental distinction arises between *conditional* and *marginal* coverage—closely related to what has been termed “relative vs. absolute uncertainty” [28] or “adaptive vs. calibrated uncertainty.” Conditional coverage requires that prediction intervals achieve the target coverage level at *every individual input*, thereby capturing *local* or *relative* uncertainty. Formally, a prediction interval $C(X_{n+1})$ satisfies conditional coverage at level $1 - \alpha$ if

$$\forall x \in \text{supp}(X) : \mathbb{P}[Y_{n+1} \in C(X_{n+1}) \mid X_{n+1} = x] \geq 1 - \alpha.$$

By contrast, *marginal coverage* only guarantees coverage *on average* over the distribution of inputs:

$$\mathbb{P}[Y_{n+1} \in C(X_{n+1})] \geq 1 - \alpha.$$

While conditional coverage implies marginal coverage, the reverse does not hold. This distinction is especially important in settings with *heteroskedasticity*, where the variability of $Y \mid X$ changes across the input space, and under *distribution shift*, where the test distribution of X differs from the training distribution. Distribution shift—such as covariate shift or domain adaptation—can render marginal guarantees unreliable since they depend on the marginal \mathbb{P}_X . In contrast, conditional coverage ensures that prediction intervals remain valid even when \mathbb{P}_X changes, provided the conditional distribution $\mathbb{P}(Y \mid X)$ remains stable. In what follows, we explore the implications of these distinctions and how they shape both the evaluation and design of uncertainty quantification methods.

H.1 Metrics and their focus

To assess the quality of predictive uncertainty, various metrics capture different aspects of coverage and adaptivity:

- **NCIW** evaluates the ranking of uncertainty—whether the method assigns wider intervals to more uncertain points—but is invariant to the overall scale. It reflects relative uncertainty without penalizing miscalibration. Minimum Negative Log-Likelihood (NLL_{\min}) [28] similarly measures relative uncertainty, focusing on whether the method correctly ranks more vs. less uncertain inputs, independent of the predicted scale.
- **Quantile Loss**, **CRPS**, and **AISL** combine both relative and absolute components. These metrics penalize both poor ranking and miscalibration, rewarding methods that adapt well to heteroskedasticity while maintaining valid coverage.
- **PICP** and **NIW** each provide only partial information: PICP measures calibration but is blind to adaptivity, while NIW captures the average scale of uncertainty. However, optimizing both jointly implicitly requires the method to rank uncertainty well and calibrate it accurately.

These metrics reflect different priorities in uncertainty quantification. Choosing among them (or combining them) depends on whether the primary goal is calibration, adaptivity, or both.

H.2 Applications

Understanding whether a method captures relative or absolute uncertainty has practical implications across a range of applications:

In **active learning**, the primary objective is to identify inputs x for which the model is most uncertain, guiding efficient data acquisition. Here, only the ranking of uncertainty matters—selecting the point with the highest epistemic uncertainty. Methods that preserve good relative uncertainty, even if miscalibrated, often suffice.

In **Bayesian optimization**, many acquisition functions (such as upper confidence bound or entropy search) depend more on relative than absolute uncertainty [107, 108]. Using upper bounds of the form $\hat{f}(x) + c$ with constant c across all x does not improve over exploiting $\hat{f}(x)$ alone, highlighting the centrality of uncertainty ranking over calibration in this setting.

In **human-in-the-loop automation**, relative uncertainty can guide prioritization—for instance, flagging uncertain cases for expert review. While calibrated intervals may not always be necessary, correct ordering of confidence can improve decision efficiency and safety.

H.3 Methods

Different uncertainty quantification methods prioritize and estimate relative and absolute uncertainty to varying degrees:

- **NOMU** [28] is explicitly designed to estimate only relative uncertainty. It does not attempt to calibrate the absolute scale, making it suitable for applications where ranking matters but calibrated intervals are unnecessary.
- **Deep ensembles** [22] typically yield strong performance in capturing relative uncertainty, particularly through diversity in predictions across ensemble members. However, they often suffer from miscalibration in the absolute scale of uncertainty unless explicitly corrected.
- **CLEAR** separately estimates relative epistemic and aleatoric uncertainty and combines them using a tunable parameter λ , which also refines the ranking of uncertainty—offering an alternative to standard calibration techniques. The absolute scale is then calibrated using a second parameter, γ_1 , allowing for flexible control over both adaptivity and calibration.

These methods highlight the spectrum of approaches to uncertainty quantification, from ranking-only models to fully calibrated systems.

H.4 Calibration Techniques

The absolute scale of uncertainty is critical in applications where the expected risk or cost over a population matters. For example, in probabilistic risk management, climate forecasting, or decision-making under uncertainty, one needs valid estimates of average confidence. However, as emphasized by pathological cases that achieve perfect PICP with no adaptivity, relative uncertainty remains essential for practical utility. Several approaches have been developed to adjust the scale of uncertainty estimates while preserving different structures:

- **Multiplicative calibration** scales all predictions by a constant factor, preserving the multiplicative structure of uncertainty. This is appropriate when the model’s ranking is reliable.
- **Additive calibration** shifts all intervals uniformly, preserving additive differences but potentially distorting proportional uncertainty.
- **Isotonic calibration** [3] applies a nonparametric monotonic transformation that preserves the ranking of uncertainty, suitable when only order is trusted.
- **CLEAR** calibrates aleatoric and epistemic uncertainty separately, allowing independent yet coherent control of both components. This facilitates calibrated estimates of total predictive uncertainty while preserving the relative structure.

H.5 Achieving Conditional Coverage

Achieving conditional coverage requires addressing both components of predictive uncertainty:

1. Estimating relative uncertainty accurately—capturing how uncertainty varies across inputs.
2. Calibrating the absolute scale to ensure the desired coverage level holds at each input.

Even when conditional coverage is not required, improving relative uncertainty tends to reduce average interval width and improve marginal calibration. Thus, adaptivity and calibration are not mutually exclusive but can reinforce one another.

CLEAR is explicitly designed to target both forms of uncertainty—modeling and calibrating relative and absolute epistemic, aleatoric, and total predictive uncertainty. As such, it provides a flexible and principled framework for applications demanding both adaptivity and reliability.